Aus dem

Department für Diagnostische Labormedizin der Universität Tübingen

Institut für Medizinische Mikrobiologie und Hygiene

Analysis and comparison of different methods for the quantification of alginate produced by Pseudomonas aeruginosa

Inaugural-Dissertation
zur Erlangung des Doktorgrades
der Medizin

der Medizinischen Fakultät
der Eberhard Karls Universität
zu Tübingen

vorgelegt von

Uhl, Damaris Annika

2024

Dekan: Professor Dr. B. Pichler

1. Berichterstatter: Privatdozent Dr. E. Bohn
2. Berichterstatter: Professor Dr. C. Stein-Thoeringer

Tag der Disputation: 12.09.2024

Content

Figures

Tables

Equations

Abbreviations

ATP	adenosine triphosphate
cAMP	cyclic adenosine monophosphate
CF	cystic fibrosis
CFTR	cystic fibrosis transmembrane conductance regulator
d	day(s)
ENaC	epithelial sodium channel
FA	formaldehyde
FT-IR	Fourier transform infrared spectroscopy
h	hour(s)
IL1-β	Interleukin-1 beta
LB	lysogeny broth
LPS	lipopolysaccharide
min	minute(s)
ml	milliliter
μl	microliter
nm	nanometer
mm	millimeter
OD	optical density
OMV	outer membrane vesicle
P. aeruginosa	*Pseudomonas aeruginosa*
PBS	phosphate-buffered saline
rpm	revolutions per minute
RT	room temperature
TNF-α	tumor necrosis factor alpha
WHO	world health organization

1 Introduction

1.1 Cystic fibrosis

Cystic fibrosis (CF) is an autosomal recessive genetic disease (Kerem et al., 1989) that is caused by mutations in the gene encoding the Cystic Fibrosis Transmembrane Conductance Regulator (CFTR) (Riordan et al., 1989). It is the most frequent fatal genetic illness in the Caucasian population (O'Sullivan & Freedman, 2009) with a prevalence of approximately 1:2500 and a carrier frequency of approximately 1:25 (Alton et al., 2016). As CFTR is expressed in various tissues, multiple organ systems are affected by CF, particularly the lung, but also the pancreas, liver, gastrointestinal system, and the reproductive organs (Alton et al., 2016; Davis, 2006). Frequent symptoms include meconium ileus in newborns, increased levels of sweat chloride, respiratory symptoms, failure to thrive and male infertility (Davies et al., 2007; Davis, 2006). Pulmonary disease is the most severe component of CF and a major contributor to lethality (O'Sullivan & Freedman, 2009; Sommerburg & Mall, 2022). It manifests itself mainly through wheeze, cough and lower airway infections such as pneumonia that aggravate with time, resulting in hypoxemia and hypercarbia (Alton et al., 2016; Davies et al., 2007; O'Sullivan & Freedman, 2009). Common manifestations of upper airway disease involve sinusitis and nasal polyps (Alton et al., 2016; Davies et al., 2007). Pancreatic symptoms of CF include pancreatic insufficiency, which leads to vitamin deficiency and subsequent diseases such as osteoporosis, steatorrhea and malnutrition, and diabetes mellitus caused by obstruction of intrapancreatic ducts (O'Sullivan & Freedman, 2009).

In the 20th century, CF was mainly a disease of children due to the severity of the symptoms, the dominating life-limiting factor being pulmonary infection (Davis, 2006). The life expectancy of CF patients has increased in the last decades, from about 6 months to 50 years or more predicted for children born in the early 2000's (Davis, 2006; O'Sullivan & Freedman, 2009). This has been accomplished due to new insights, infection treatment, nutritional management, and new medications such as CFTR modulators (Elborn, 2016; Griese et al., 2021).

Especially CFTR modulators, such as the combination of Elexacaftor, Tezacaftor and Ivacaftor, showed remarkable clinical effectiveness, improving several clinical parameters (Griese et al., 2021). However, decline in lung function remains the most important life-limiting factor, showing the potential that lies in CF lung infection research (Davis, 2006; Sommerburg & Mall, 2022).

1.2 Pathophysiology of cystic fibrosis

More than 2000 genetic CFTR mutations have been identified and categorized according to the severity of CFTR impairment, disease manifestations and treatment options (Alton et al., 2016; Marson et al., 2016; Wang, 2017). However, some mutations do not lead to the disease since a functional protein is still expressed (Alton et al., 2016). CFTR is located in the apical membrane of epithelial cells and belongs to the family of cAMP dependent ATP binding cassette transporters (Bhagirath et al., 2016). It acts as an ion channel as well as a regulator for other channels such as the epithelial sodium channel ENaC (Bhagirath et al., 2016; Mehta, 2005; Quinton, 2010).

Regarding the ion channel activity, CFTR transports Cl^- ions in luminal direction (Sommerburg & Mall, 2022). Additionally, CFTR serves as an inhibitor for ENaC, which absorbs sodium into the respiratory epithelium (Kunzelmann, 2003). The absorption of sodium is followed by the diffusion of H_2O (Sommerburg & Mall, 2022). In healthy lungs, an aqueous periciliary fluid layer of circa 6 μm is formed, on which lies a mucus layer that traps inhaled particles such as bacteria (Pape et al., 2023; Vogelberg & Seidenberg, 2022). The mucus layer is moved towards the pharynx by a coordinated stroke of the cilia that are freely movable in the periciliary layer (Vogelberg & Seidenberg, 2022). This process is called mucociliary clearance and responsible for effective cleansing of the airways (Pape et al., 2023; Vogelberg & Seidenberg, 2022) (Figure 1).

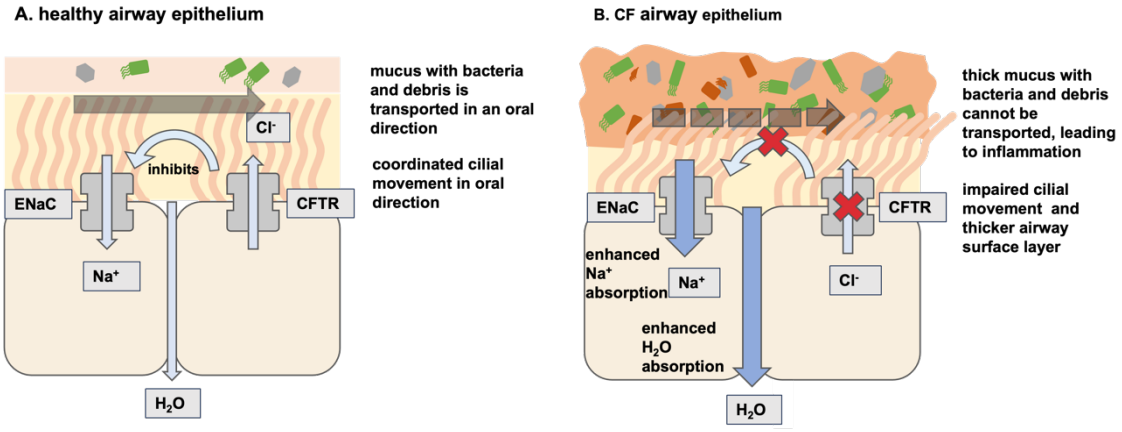

Figure 1: Mucociliary clearance in healthy and CF airways
1A, mucociliary clearance of healthy airways. Chloride is secreted into the lumen by CFTR and sodium absorption through ENaC is inhibited by CFTR (Kunzelmann, 2003; Sommerburg & Mall, 2022). H_2O absorption is low and the cilia, surrounded by the liquid periciliary fluid, form a coordinated stroke in oral direction (Lüllmann-Rauch & Asan, 2019). Bacteria and other inhaled particles are transported out of the airways with the mucus (dark grey arrow) (Lüllmann-Rauch & Asan, 2019).
1B, mucociliary clearance of airways impaired by CF. Chloride secretion is reduced due to a defective CFTR (Sommerburg & Mall, 2022). Na^+ and H_2O absorption are increased, leading to a dehydrated airway surface (Sommerburg & Mall, 2022). The ciliary movement is impaired by the dehydration of the airway surface liquid and a thick sticky mucus forms (Alton et al., 2016; Herzog et al., 2004; Matsui et al., 1998; Sommerburg & Mall, 2022). Therefore, bacteria and other inhaled particles cannot be transported in oral direction. Due to impaired mucociliary clearance and defective bactericidal activity in the airway surface liquid, bacterial colonization and chronic inflammation develop (Bhagirath et al., 2016; Govan & Deretic, 1996; Matsui et al., 1998).

A defective CFTR leads to reduced epithelial chloride secretion into the lumen and elevated sodium resorption, which leads to enhanced sodium-associated water absorption, which then again leads to dehydration of the airway surface, and impaired mucociliary clearance (Figure 1) (Alton et al., 2016; Herzog et al., 2004; Sommerburg & Mall, 2022). Therefore, pathogens cannot be sufficiently transported out of the lung, which causes airway colonization and chronic infection (Govan & Deretic, 1996; Matsui et al., 1998). Furthermore, bactericidal activity in the airway surface liquid of CF patients is impaired because of high salt concentrations (Joris et al., 1993; Smith et al., 1996). This also leads to bacterial colonisation and chronic inflammation (Bhagirath et al., 2016). Moreover, a different lung environment contributes to bacterial colonization: Long et al. showed that even very young CF patients with little symptoms have structural abnormalities of the airways such as thickened walls and increased airway diameter (Long et al., 2004).

1.3 *P. aeruginosa* infection

Pseudomonas aeruginosa (*P. aeruginosa*) is an opportunistic pathogen that frequently causes severe infections in immunocompromised patients, ventilated patients, and patients with pre-existing respiratory conditions, such as CF (Kipnis et al., 2006). It is an environmental, facultative anaerobic, Gram-negative, rod-shaped bacterium and the predominant pathogen in adult CF patients nowadays (Bhagirath et al., 2016; Hassett et al., 2009). 43 % of CF patients were infected with *P. aeruginosa* in 2019, the median age of the first infection being 5 years (Cystic Fibrosis Foundation, 2019).

As *P. aeruginosa* is frequently resistant to antibiotics, it poses a great risk to our healthcare system and was defined as one of the six ESKAPE pathogens for which the development of new antibiotics is most urgent (Mulani et al., 2019; Qin et al., 2022). *P. aeruginosa* features a multitude of virulence mechanisms of which only a very brief overview can be given in this work (Qin et al., 2022). To begin with, *P. aeruginosa* produces lipopolysaccharide (LPS), a component of its outer membrane (Qin et al., 2022). It protects the outer membrane of the bacterium, damages host cells, and possibly contributes to antibiotic tolerance (Qin et al., 2022). Furthermore, it acts pro-inflammatory by inducing the production of proinflammatory cytokines like tumor necrosis factor alpha (TNF-α) and interleukin-1 beta (IL1-β) (Qin et al., 2022). Another outer membrane associated virulence mechanism are so-called outer membrane vesicles (OMVs), which can release various bacterial proteins and nucleic acids, and possibly facilitate the formation of biofilms (Qin et al., 2022). *P. aeruginosa* possesses different secretion systems, which secrete for example proteases and cytotoxins into the extracellular milieu or into host cells (Qin et al., 2022). Furthermore, *P. aeruginosa* can form biofilms by producing the exopolysaccharides alginate, Pel and Psl, after surface attachment by flagella and pili (Qin et al., 2022). These biofilms impede the defense mechanisms of the host (such as phagocytosis) and further increase antibiotic tolerance (Hassett et al., 2009; Qin et al., 2022).

In CF patients, an acute *P. aeruginosa* infection becomes chronic by applying several adaptation mechanisms and genetic changes. *P. aeruginosa* colonies from chronically infected lungs can develop a hypermutator phenotype, unlike *P.*

aeruginosa isolated from early infected lungs (Häussler, 2010; Hogardt & Heesemann, 2010). Due to mutations in regulatory genes leading to excessive alginate synthesis, *P. aeruginosa* can switch to a mucoid phenotype during chronic infection (Hassett et al., 2009). Furthermore, *P. aeruginosa* isolated from chronically infected lungs often exhibits antibiotic resistances caused by mutations and an adapted metabolism (Hassett et al., 2009). As shown by Frederiksen et al., the onset of chronic *P. aeruginosa* infection can be delayed by aggressive antibiotic treatment, which preserves lung function (Frederiksen et al., 1997). The development of a chronic infection, which contributes to morbidity and mortality, however, cannot be prevented (Costerton et al., 1999; Cramer et al., 2023; Hassett et al., 2009). Cramer et al. showed that the lungs of CF patients are usually colonized by a single *P. aeruginosa* clone (Cramer et al., 2023). This clone genetically diversifies over time, expressing different phenotypes (Cramer et al., 2023). These variants can express for example enhanced antibiotic resistance as well as increased production of exopolysaccharides, leading to the formation of biofilms (Govan & Deretic, 1996; Häussler, 2010). Bacteria located in biofilms can show an up to 1000-fold increase in antibiotic tolerance compared to their genetically identical planktonic counterparts (Häussler, 2010). This is likely due to the biofilm matrix acting as a diffusion barrier for antibiotics, as well as a slower metabolism of sessile bacteria (Häussler, 2010). *P. aeruginosa* can produce at least three different types of exopolysaccharides: Psl, Pel and alginate, of which alginate is almost exclusively produced by *P. aeruginosa* from chronically infected CF lungs (Franklin et al., 2011). With the overproduction of alginate, the conversion from a non-mucoid to a mucoid phenotype of *P. aeruginosa* is accomplished (Bragonzi et al., 2005; Hogardt & Heesemann, 2010). Mucoidy is a hallmark of chronic CF infections (Hogardt & Heesemann, 2010). As a mucoid phenotype is related with poorer outcome and impaired lung function, Hogardt and Heesemann concluded that “alginate is one of the most significant virulence determinants in the context of chronic CF airway disease” (Hogardt & Heesemann, 2010).

1.4 Biofilm formation by *P. aeruginosa* in the cystic fibrosis lung

As described above, conversion to an alginate overproducing, mucoid phenotype is the hallmark of chronic *P. aeruginosa* infection (Hogardt & Heesemann, 2010). In the lungs of CF patients, *P. aeruginosa* can evolve from its planktonic state and form biofilms (Costerton et al., 1999). Microscopic observations of CF sputum samples as well as studies of quorum sensing signals support this hypothesis (Singh et al., 2000). As mentioned, *P. aeruginosa* in biofilms is impossible to permanently eradicate and highly tolerant to antimicrobial agents (Costerton et al., 1999; Nikaido, 1994). One reason for this is that the biofilm matrix can act as a physical barrier (Costerton et al., 1999; Häussler, 2010). Another reason is that alginate is negatively charged prevent charged antibiotics from diffusing through the biofilm (Aitken et al., 2011). Marcus and Baker showed that mucoid *P. aeruginosa* adheres to hamster tracheas 10- to 100-fold better than nonmucoid *P. aeruginosa* which indicates the importance of mucoidy for chronic *P. aeruginosa* infection (Marcus & Baker, 1985). Furthermore, alginate alters the structure of biofilms, leading to thicker biofilms (Nivens et al., 2001).

1.5 Genetic and posttranslational regulation of alginate expression

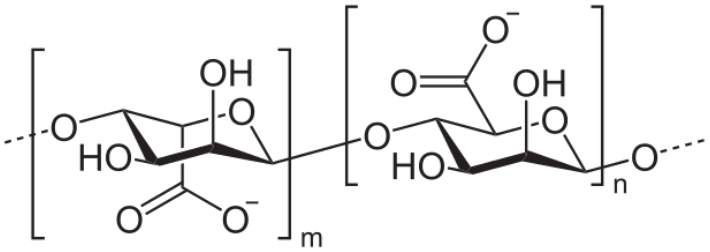

Figure 2: Structure of alginate
Alginate is a negatively charged polysaccharide consisting of β-D-mannuronate and α-L-guluronate (Gacesa, 1988; Hay et al., 2014; Pier et al., 2001).(NEUROtiker via Wikimedia Commons, 2008)

As described above, alginate production is a marker for chronic *P. aeruginosa* infection. Since chronic infections with *P. aeruginosa* cannot be permanently eradicated and contribute to CF morbidity and mortality, further research of this polysaccharide is of great importance. Alginate is an anionic linear polysaccharide consisting of β-D-mannuronate and its epimer α-L-guluronate in varying order (Figure 2) (Gacesa, 1988; Hay et al., 2014; Pier et al., 2001). It is

produced by seaweeds and a few bacteria (Liu et al., 2019). The chemical structure of alginate differs between bacterial and seaweed alginate (Ashby, 1994). Bacterial alginate has a more complex structure and contains more mannuronate than seaweed alginate (Ashby, 1994; Pritchard et al., 2023). Alginate produced by *P. aeruginosa* is O-acetylated, changing its biological characteristics and reducing recognition by the host immune system, such as biofilm structure (Nivens et al., 2001; Pier et al., 2001). It is a large molecule, and the regulation of its biosynthesis is complex (Wang, 2017). Chitnis and Ohman identified the alginate biosynthesis gene cluster comprising 12 genes (Chitnis & Ohman, 1993). Expression of these genes is regulated by *AlgU*, which is itself encoded by a gene located in an operon containing the regulatory genes *MucA*, *MucB*, *MucC* and *MucD* (Hay et al., 2014). According to the findings of Mathee et al, mutations in *MucA* for example lead to overexpression of the alginate biosynthesis genes and mucoidy (Mathee et al., 1999). However, there is evidence that in addition to mutations, alginate production can be increased by regulation and external stimuli, for example cell stress (Schmidt et al., 2016). Schmidt et al. identified that the diguanylate cyclase *sadC*, which produces the signalling molecule cyclic c-di-GMP, promotes alginate expression in non-mucoid *P. aeruginosa* and is more active in low oxygen tensions (Schmidt et al., 2016). Alginate production increased within minutes as a reaction to oxygen depletion, when the bacteria were not yet growing biofilms (Schmidt et al., 2016). The stimulation of alginate synthesis by c-di-GMP is supported by the fact that an essential component of the alginate biosynthesis machinery contains a PilZ domain that are known to bind c-di-GMP (Merighi et al., 2007). However, alginate levels were not as high as in mucoid isolates carrying mutations constitutively overexpressing the alginate biosynthesis gene cluster (Schmidt et al., 2016). As *P. aeruginosa* strains carrying a *sadC* deletion produced lower amounts alginate under anaerobic conditions, *sadC* seems to be an important stimulator of alginate production under anaerobic conditions (Schmidt et al., 2016). The finding that c-di-GMP production by purified *sadC* is increased under anaerobic conditions supports this finding (Schmidt et al., 2016). Since hypoxic and anaerobic conditions are present in the lung of CF patients increased alginate synthesis by

non-mucoid *P. aeruginosa* isolates during early stages of infection could be an important adaptive mechanism (Hassett et al., 2009; Schmidt et al., 2016). To elucidate the role of *sadC* and the regulatory pathways involved it is thus necessary to measure intermediate changes in alginate levels.

1.6 Methods of alginate detection

Analyzing the intermediate changes in alginate levels upon environmental stimuli, it is required to use a sensitive detection method. However, methods of alginate measurement have been developed, mostly for mucoid versus non-mucoid *P. aeruginosa,* and are based on enriched but not purified alginate. The first method was the carbazole assay, which was first described by Zacharias Dische and modified several times (Bitter & Muir, 1962; Dische, 1947; Knutson & Jeanes, 1968). Furthermore, different immunofluorescent and chromatographic assays were developed (Awad & Aboul-Enein, 2013; Garner et al., 1990). Alginate is a very complex polysaccharide and of a high molecular weight (Awad & Aboul-Enein, 2013). The structure of alginate produced by *P. aeruginosa* differs from the structure of commercially available sodium alginate, which is usually derived from seaweeds (Ashby, 1994; Wang, 2017). This complicates the measurement of alginate produced by *P. aeruginosa*, as it is required to enrich the alginate for most established assays, which is a challenging task for polysaccharides involving many steps (Zheng et al., 2016). Dusseault et al. showed that contamination of commercial alginate, especially by proteins, cannot be eliminated completely by purification (Dusseault et al., 2006). The abundance of available assays of alginate measurement alone further supports the thesis that alginate produced by *P. aeruginosa* is incredibly difficult to precisely measure (Awad & Aboul-Enein, 2013; Wang, 2017). In the following paragraphs, four methods of alginate detection will be presented: Two established methods of alginate detection and two more recent methods that were explored in detail for this work.

1.6.1 Carbazole assay

The carbazole assay war one of the first established methods to measure alginate concentrations and is still applied frequently today. It was first described by

Zacharias Dische for the quantification of uronic acid, other substances containing hexuronic acids were also tested (Dische, 1947). This test is based on the reaction of sugars with concentrated mineral acids, the products of which react with certain organic substances to produce a colour (Dische, 1947). In the following paragraph, the original experimental procedure by Zacharias Dische will be described. A solution containing uronic acid (e.g. alginate) was heated together with concentrated sulfuric acid, cooled down and an alcoholic solution of carbazole is added (Dische, 1947). A pink colour appeared and could be measured photometrically at a wavelength of 530 nm (Dische, 1947). The assay was modified by several researchers such as Knutson and Jeanes, for example by adding borate to the sulfuric acid reaction and changing the heating temperature, which increased the specificity for D-mannuronic acid, a component of bacterial alginate (Knutson & Jeanes, 1968). The carbazole assay does not require special devices and can be performed in most labs. It is frequently used for the determination of the alginate content of mucoid *P. aeruginosa* isolates (Ahmar et al., 2020; Zheng et al., 2016). Disadvantages of the carbazole assay include the low specificity due to the interference of other substances, e.g. proteins, sugars and salts, hence it is necessary to purify the samples as far as possible (Dische, 1947; Frazier et al., 2008; Zheng et al., 2016). The assay involves strong, hazardous chemicals including concentrated sulfuric acid which must be handled cautiously (Ahmar et al., 2020). Furthermore, due to the nature of the experimental set-up, it is not possible to observe the bacteria on the single cell level.

1.6.2 Immunofluorescence assay

Garner et al. developed a murine antiserum against *P. aeruginosa* mucoid exopolysaccharide for the purpose of evoking the production of antibodies against *P. aeruginosa* alginate (Garner et al., 1990). Based on their findings, an indirect immunofluorescence assay for measuring lower levels of alginate was developed as a procedure (Bragonzi et al., 2005; Schmidt et al., 2016; Theilacker et al., 2003). Bacteria were incubated with anti-alginate rabbit serum after being fixed with formaldehyde, washed, and blocked with goat serum (Schmidt et al., 2016; Theilacker et al., 2003). The rabbit serum was cultivated against purified

alginate obtained from mucoid *P. aeruginosa* and incubated with non-mucoid *P. aeruginosa* that was lyophilized and fixed by formaldehyde (Schmidt et al., 2016). A Cy3-conjugated goat anti-rabbit antibody was applied, and DNA was stained with 4,6-diamidino-2-phenylindole (Schmidt et al., 2016). The samples were viewed under an epifluorescence microscope and the fluorescence signal was quantified (Schmidt et al., 2016). Using epifluorescence microscopy, this technique was sensitive enough to detect an intermediate increase in alginate production by a non-mucoid *P. aeruginosa* isolate (Schmidt et al., 2016). Quantification of alginate as well as observations at the single cell level were possible (Schmidt et al., 2016). Unfortunately, due to variations in rabbit antiserum batches and/or generation of the antiserum, this technique showed not be reliable.

1.6.3 Crystal violet assay

The method of aggregating alginate from *P. aeruginosa* with calcium ions and staining with crystal violet was first described by Zheng et al. (Zheng et al., 2016). This assay, unlike the carbazole assay, requires no purification of the alginate (Zheng et al., 2016). It utilizes the ability of calcium cations to form an aggregate with negatively charged alginate (Page & Sadoff, 1975). Upon mixing Ca^{2+} ions with purchased alginate solution or the supernatant of centrifuged mucoid *P. aeruginosa* liquid culture, a macroscopically visible aggregate was observed, whereas no aggregate was present after mixing Ca^{2+} with LB medium and wildtype *P. aeruginosa* (Zheng et al., 2016). These aggregates were stained with crystal violet. The absorbance was measured, and a standard curve was obtained by measuring concentrations of commercially available alginate (Zheng et al., 2016). According to Zheng et al., a linear correlation was observed for alginate concentrations between 0.2 and 2 mg/ml and the alginate could be measured without having to be purified or diluted, but the sensitivity was rather low for an alginate concentration below 0.2 mg/ml (Zheng et al., 2016). This method, including its sensitivity, applicability, and limitations, will be further explored in this work, as it offers a simple, quick approach without the need to handle harsh chemicals, while maintaining adequate sensitivity. It will also be tested if the

method is adequate for measuring alginate produced by non-mucoid *P. aeruginosa.*

1.6.4 Alcian blue staining

Alcian blue is a cationic dye that has been utilised for the quantification of glycosaminoglycans and glycoproteins (Frazier et al., 2008; Wardi & Allen, 1972). However, it has not yet been explored if it could be a suitable staining agent for alginate. The Alcian blue assay showed a higher sensitivity compared to the carbazole assay when quantifying glycosaminoglycans isolated from animals (Frazier et al., 2008). Other advantages include that it does not require special equipment nor very hazardous chemicals and that it can be performed in a conventional lab setting. An important benefit is that the bacteria can be analyzed on the single cell level when used in combination with microscopy: While Frazier et al. quantified the alginate by measuring the absorbance, in this work the *P. aeruginosa* bacteria were dyed and imaged under a microscope. Compared to other methods that have been mentioned in the previous paragraphs, the Alcian blue assay offers many promising aspects. In this work, it will be probed whether Alcian blue staining is applicable for the detection of alginate and for measuring the levels thereof in particular.

1.7 Aims

Chronic *P. aeruginosa* infection is a major cause of disease burden and death of CF patients (Hassett et al., 2009; Hogardt & Heesemann, 2010). Acute infection and colonisation precede chronic infection and must be treated aggressively with antibiotics in order to be eradicated (Munck et al., 2001). Once the infection has become chronic, it can hardly be eradicated (Munck et al., 2001; Winstanley et al., 2016). Chronic infection is latest determined when *P. aeruginosa* converts to a mucoid phenotype which is defined by the increased synthesis of alginate (Franklin et al., 2011; Hogardt & Heesemann, 2010). Boyd and Chakrabarty showed that alginate is an important component of the biofilm that *P. aeruginosa* forms in chronically infected lungs (Boyd & Chakrabarty, 1995). It is even constated “arguably the most important microbial virulence determinant in CF lung infections” (Govan & Deretic, 1996). Therefore, great potential lies in the research of alginate and chronic *P. aeruginosa* infection of CF patients. Production of alginate by mucoid isolates has been studied in the past, but more recently, it has been discovered that non-mucoid *P. aeruginosa* isolates can produce intermediate levels of alginate as a quick stress response (Schmidt et al., 2016). It is especially important to understand the regulatory mechanisms of alginate production and to investigate environmental signals or components such as antibiotics that lead to increased alginate production. A sensitive method to detect changes in alginate production is crucial for this aim and could ultimately enable the development of substances that inhibit alginate synthesis for the treatment of chronic *P. aeruginosa* infection. Alginate, especially alginate that is produced by *P. aeruginosa*, is a large, complex molecule that is difficult to purify (Awad & Aboul-Enein, 2013). Because of this, measuring it is a highly challenging task. To directly detect changes in alginate production, it is helpful to be able to observe alginate production at the single cell level. For the determination of high alginate levels produced by mucoid *P. aeruginosa*, established assays exist, but they require purification or enrichment of the alginate (Østgaard, 1993; Zheng et al., 2016). Furthermore, a method to measure intermediate levels of alginate produced by non-mucoid *P. aeruginosa* is necessary. In our laboratory, the alginate content of *P. aeruginosa* samples had been measured by an

immunofluorescence assay using alginate-specific rabbit antiserum (Schmidt et al., 2016). However, this method showed variability when using different batches of antiserum. Establishing a different method for alginate measurement was therefore required.

The aim of this work was to find a sensitive method for measuring or detecting low alginate concentrations in *P. aeruginosa* cultures with different genomic backgrounds cultivated under various oxygen tensions, optimizing the conditions thereof and analysing its practicality for use in the lab. Specifically, the crystal violet assay and the Alcian blue staining method were tested. The crystal violet assay was first described by Zheng et al. (Zheng et al., 2016). It was aimed to test its reproducibility, adjust the conditions, and differentiate even little changes in alginate levels of different *P. aeruginosa* strains, if possible. The Alcian blue assay was tested for the first time for detecting alginate in *P. aeruginosa*. It was planned to establish a standard protocol for this method, explore different conditions and test its sensitivity and its limitations. Furthermore, it was explored if this assay was appropriate for observing changes on the single cell level.

Specific aims:

- Test the suitability and reproducibility of the recently published quantitative crystal violet assay for alginate using high, intermediate and low alginate producing *P. aeruginosa* strains.
- Test the suitability of the Alcian blue dye for detecting alginate on *P. aeruginosa* cells using microscopy.

2 Materials and methods

2.1 Devices

Table 1: Devices used in this work

Device	Description	Manufacturer
Centrifuge	Multifuge 35-R	Heraeus
Freezer -80°C		Stirling Ultracold
Incubator	Kelvitron®t	Heraeus
Microscope	BX51	Olympus
Photometer	BioPhotometer D30	Eppendorf
Pipette	Eppendorf Reference	Eppendorf
Pipette	Eppendorf Research	Eppendorf
Pipette (multichannel)	Discovery Comfort (200 µl)	ABIMED
Pipet controller	Accu-jet® pro	Brand
Platform shaker	Unimax 1010	Heidolph
Precision scale	Kern PCB 1000-2	KERN & SOHN
Refrigerator		LIEBHERR
Shaking incubator	MaxQ 4450	Thermo Fisher Scientific
Sterile bench	HeraSafe KS18	Thermo Fisher Scientific
Tabletop centrifuge	Eppendorf Centrifuge 5415 R	Eppendorf
Tecan Reader	Infinite® M200 PRO	TECAN
Tecan Reader	Spark®	TECAN
Vortexer	REAX Control	Heidolph

2.2 Media

Table 2: Media used in this work

Product	Components	Amount used for 500 ml
LB medium	Tryptone Yeast extract NaCl H_2O	5 g 2.5 g 5 g Fill up to 500 ml, Autoclave
LB agar	Lysogeny broth (LB) Agar H_2O	7.5 g 10 g Fill up to 500 ml Autoclave

Modified M9 agar	Bacto Agar yeast extract H_2O 100 mM KNO_3 5x M9 salts: Na_2HPO_4 n KH_2PO_4 NaCl NH_4Cl Sterile 25% glucose 0,1 M $CaCl_2$ 1 M $MgSO_4$	7.5 g 50 mg Water up to 290 ml 100 ml Autoclave 100 ml 30.0 g 15.0 g 2.5 g 5.0 g 10 ml 50 µl (filter sterilize) 0.2 ml (filter sterilize)
Freezing medium	LB medium + 15% glycerol	

2.3 Chemicals

Table 3: Chemicals used in this work

Product	**Manufacturer**
Acetic acid	VWR chemicals
Alcian blue solution	EMD millipore
Bacto™ Agar	Becton, Dickson and Company (#214010)
Bacto™ yeast extract	Becton, Dickson and Company (#212750)
Calcium chloride dihydrate	AppliChem GmbH
Calcium chloride tetrahydrate	Merck KGaA
Crystal violet	SERVA
H_2O	Ampuwa Fresenius Kabi
Glucose	Sigma
KNO_3	Merck KGaA
$MgSO_4$	Sigma-Aldrich
Sodium alginate	Sigma-Aldrich
PBS buffer	Gibco
Formaldehyde 37%	Sigma-Aldrich

2.4 Consumables

Table 4: Consumables used in this work

Product	Description	Manufacturer
15 ml tube	Cellstar® tubes	Greiner bio-one (#1 88271)
50 ml tube	50 ml Polypropylene Conical Tube	Falcon (#352070)
96-well plate	Cellstar®	Greiner bio-one
96-well plate	Flat bottom	Thermo Scientific
Anaerobic gas generating sachets	Oxoid™ AnaeroGen™ 2,5 l	Thermo Scientific
Anaerobic indicator strips	Anaerotest	Merck KGaA
Bottle filters	Bottle top filter	Corning
Cryo tubes	CryosTM, PP, with screw cap, sterile	Greiner bio-one (#126263)
Culture tubes	14 ml Polystyrene Round Bottom Tube	Falcon (#352051)
Cuvettes	Semi-micro cuvette	Sarstedt
Desinfectant	Descosept AF	Dr. Schuhmacher (#00-311)
Garbage bags	PP disposal bags	BRAND
Nitril gloves	Nitrile, powderfree medical examination gloves	ABENA (#290418)
Precision wipes	KIMTECH SCIENCE® Precision Wipes Tissue Wipers	Kimberly-Clark Professional (#05511)
Serological pipette	Corning incorporated costar stripette (5/ 10/ 25/ 50 ml)	Sigma-Aldrich (#CLS4051/ CLS4101/ CLS4251/ CLS4501)
Syringe	Combitips plus 10 ml	Eppendorf
Syringe filter (pore size: 0,2 µm)	Acrodisc® Syringe Filters	Pall
Syringe	Injekt® 10 ml	Braun (#4606108 V)
Syringe	Injekt® 20 ml	Braun (#4606205 V)
Glass slides		Langenbrinck
Poly-D-Lysine coverslips		Neuvitro
24-well plate		Greiner

2.5 Bacterial strains

Table 5: Bacterial strains used in this work

Name	Description	Reference
PAO1 wildtype	*P. aeruginosa,* non-mucoid type strain (chronic wound isolate)	Holloway, 1955
PDO300	mucA22 mutant of *P. aeruginosa* PAO1; mucoid phenotype,	Mathee et al., 1999
PAO1Δ*sadC*	unmarked in-frame deletion of full length s*adC*	Schmidt et al., 2016
PAO1s*adC*ΔTM	cytoplasmic domain containing the GGDEF motif expressed, only upstream transmembrane domains are deleted	Schmidt et al., 2016

2.6 Software

Table 6: Software used in this work

Software	Manufacturer
Microsoft Office 2016	Microsoft Corporation
Microsoft Office 2010	Microsoft Corporation
Tecan i-control 2.0	TECAN
Tecan SparkControl™	TECAN
Adobe Photoshop CS6	Adobe systems
GIMP 2.6	
R	R Core Team

2.7 Cultivation of the bacteria

2.7.1 Agar plate cultures

P. aeruginosa from cryogenic stock or plate culture was grown on lysogeny broth (LB) or modified M9 agar plates (henceforth termed M9) and incubated at 37°C. Anaerobic cultures were prepared using an anaerobic jar with an airtight lid and an anaerobic gas sachet. An anaerobic indicator strip was placed in the jar. The cultures were incubated at 37°C for approximately 48 h.

2.7.2 Liquid cultures

From cryogenic stock liquid cultures were prepared using 2 ml LB medium. The cultures were incubated overnight at 37°C and 200 rpm. If required, bacteria were cultured in a 100 ml or 250 ml Erlenmeyer flask using 25 or 50 ml of LB medium. Those cultures were prepared from overnight cultures, inoculated at an optical density at 600nm (OD_{600}) of 0.05 and incubated overnight at 37°C and 200 rpm. Anaerobic cultures were incubated in an anaerobic jar with an airtight lid. One 250 ml or two 100 ml Erlenmeyer flasks, one anaerobic gas sachet and an anaerobic indicator strip were placed into an anaerobic jar and incubated overnight at 37°C and 200 rpm to prevent biofilm formation.

2.7.3 Preparation of cryogenic stocks

Overnight cultures of *P. aeruginosa* (see 2.7.2) were centrifuged at 3000 rpm for 3 min and the supernatant was discarded. The pellet was resuspended in LB supplemented with 15% glycerol and stored at -80°C.

2.8 Crystal violet staining

Crystal violet staining was performed according to Zheng et al., however, minor changes were made, as mentioned in the following paragraphs (Zheng et al., 2016). Instead of using a glass rod to preserve the alginate during the washing process, the alginate from the falcon tubes was pipetted or poured. The Ca-alginate complex was washed six times in total, three times before adding crystal violet and three times afterwards. Before adding crystal violet, sterilized H_2O was used to wash the alginate, after adding crystal violet, a 1% acetic acid solution was used. Alginate resuspended in LB was utilised for the preparation of the standard curves, as the bacteria would be cultured in LB medium as well. By adding Ca^{2+} ions to sodium alginate, an aggregate formed. This aggregate could then be stained with crystal violet and be quantified photometrically. First, it was explored if alginate could be precipitated by $CaCl_2$. For this, 2 mg/ml sodium alginate solution was added to 60 mM $CaCl_2$. Different concentrations of $CaCl_2$ were tested and 1 M $CaCl_2$ was utilized in further experiments.

2.8.1 Preparation of a standard curve

In order to be able to determine unknown concentrations of alginate, a standard curve was prepared with commercially available sodium alginate dissolved in sterile H_2O as well as in LB medium. Sodium alginate solutions of different concentrations (0.2 mg/ml; 0.4 mg/ml; 0.6 mg/ml; 0.8 mg/ml; 1.0 mg/ml; 1.2 mg/ml; 1.4 mg/ml; 1.6 mg/ml; 1.8 mg/ml; 2.0 mg/ml) were prepared by diluting a 2.0 mg/ml stock solution. LB and H_2O were used as negative control. 2 ml of each concentration was added to a 15 ml falcon tube containing an equal volume of 1 M $CaCl_2$ tetrahydrate aqueous solution. After that, the calcium alginate complex was washed. Different washing conditions were tested, and the most suitable ones were applied to the standard protocol. The samples were centrifuged at 2000 rpm for 5 min and the supernatant was discarded by pouring. Then the samples were washed three times by adding 2 ml of sterile water, shaking and centrifuging at 2000 rpm for 5 min at room temperature. The supernatant was discarded by pouring. In order to sufficiently saturate the alginate with dye, 2 ml of 0.3% crystal violet aqueous solution (differing from Zheng et al., 2016, who used 500 µl) was added to each of the falcon tubes and mixed until all the alginate was soaked by the crystal violet. Then the samples were incubated for 20 min at room temperature on a rotating plate. To wash the stained alginate, different conditions were tested again, and the most suitable ones were applied in the following experiments.

The falcon tubes containing stained alginate were centrifuged at 2000 rpm for 5 min, then at 3000 rpm for 5 min and the supernatant was discarded by pouring. Then the stained alginate was washed by adding 2 ml 1% acetic acid, shaking vigorously, centrifuging at 3000 rpm for 5 min and discarding the supernatant by pouring. The dye was eluted by adding 2 ml of 100% acetic acid and gentle shaking. The samples were centrifuged at 3000 rpm to get rid of clumps. The supernatant was diluted with H_2O and the resulting samples were transferred on a 96 well plate. The absorbance was measured with a plate reader at 600 nm. Samples of correspondingly acetic acid diluted with H_2O were measured as blank values and the value was subtracted from the absorbance of the crystal violet eluate.

2.8.2 Crystal violet staining of P. aeruginosa culture supernatants

Bacterial cultures were prepared and centrifuged at 4000 rpm for 20 min. 20 ml of $CaCl_2$ was poured into 50 ml tubes and 20 ml of the supernatant of the bacterial cultures was added using a serological pipette. If the culture volume was 50 ml, the supernatant was split into two falcons to test reproducibility. The samples were processed according to the standard curve protocol, starting with the alginate / $CaCl_2$ washing.

2.8.3 Statistical analysis

The statistical analysis was performed by Dr. Ulrich Schoppmeier, Institute of Medical Microbiology and Hygiene, University Hospital Tübingen.

The statistical software R was used for the analysis. The data of three independent standard curves were plotted into a diagram. Then, various polynomials were fitted to the data, e.g. a polynomial of third degree of the following form:

$$p_3(x) = a_0 + a_1 \times x + a_2 \times x^2 + a_3 \times x^3$$

Equation 1: Polynomial of third degree

A polynomial of second degree of the following form was fitted as well:

$$p_2(x) = a_0 + a_1 \times x + a_2 \times x^2$$

Equation 2: Polynomial of second degree

Standard error, a t-test and its p-value were calculated.
Moreover, a linear regression of the following form was established:

$$p_1(x) = a_0 + a_1 \times x$$

Equation 3: Linear regression

Standard error, t-test as well as p-value were calculated. Furthermore, confidence bands were calculated. The confidence bands define the region enclosing 95% of the fitted second-degree polynomials of the crystal violet standard curves, if the experiment had been performed many times. Additionally, prediction bands were calculated. These bands define the region that

encompasses 95% of sample points of the crystal violet standard curves – if the experiment had been replicated many times.

2.9 Alcian blue staining

2.9.1 Alcian blue staining on glass slides and heat fixation

For Alcian blue staining, the following growth conditions were used: LB broth, aerobic LB agar plate, aerobic M9 agar plate and anaerobic M9 agar plate. A small amount of the bacteria was transferred from the culture to a microcentrifuge tube and suspended in 0.5 ml sterile H_2O by pipetting and occasionally vortexing. Different washing conditions were tested: The bacteria were centrifuged at 3000 or 5000 rpm for 3 or 5 min, the supernatant was removed with a micropipette and resuspended in sterile H_2O. When removing the supernatant without removing some of the bacteria was impossible, the samples were centrifuged once more. 100 µl of the bacterial solution was transferred onto a glass slide, spread out, dried at room temperature and heat fixed. The bacteria were stained with Alcian blue solution that was freshly prepared by diluting the Alcian blue stock solution 1:10 with H_2O. The slides were imaged under an Olympus BX51 microscope with an oil 100x objective (NA 1.30).

2.9.2 Alcian blue staining with glass slides and formaldehyde

P. aeruginosa grown as aerobic LB, aerobic M9 and anaerobic M9 plate cultures were transferred to a microcentrifuge tube with a 1 ml pipette tip and suspended in 4% formaldehyde in phosphate-buffered saline (PBS). 100 µl of the samples was spread out on a glass slide and dried. The bacteria were stained with 10% Alcian blue solution for 1 min, washed with PBS, dried and viewed under an Olympus BX51 microscope with an oil 100x (NA 1.30) or 60x objective (NA 1.42).

2.9.3 Alcian blue staining of P. aeruginosa on coverslips

For Alcian blue staining on poly-D-lysine coated coverslips, bacteria grown on aerobic LB plates, aerobic M9 plates and anaerobic M9 plates were used. Bacteria were removed from the plate with a 1 ml pipette tip and suspended in a microcentrifuge tube containing 500 µl 4% formaldehyde PBS. Poly-D-lysine-

coated coverslips were put into 24-well plates and the bacterial suspension was added. The bacteria were centrifuged for 5 min at 1000 g and incubated at room temperature (RT) for 15 min. The bacteria were stained with freshly prepared 10% Alcian blue solution for 1 min and washed twice with 500 µl sterile H_2O. The coverslips were mounted on glass slides with 1 drop glycerol or another mounting medium and viewed under an Olympus microscope with an oil 60x and 100x objective.

3 Results

3.1 Colony morphology of a non-mucoid and a mucoid *P. aeruginosa* isolate

The *P. aeruginosa* PAO1 wildtype isolate, which is non-mucoid and produces no alginate under aerobic conditions, and the alginate overexpressing mutant *P. aeruginosa* PDO300 were grown on LB agar plates under aerobic conditions to analyze the colony morphology.

Figure 3 shows these two strains, grown on LB agar plates for 20 hours under aerobic conditions. Several single colonies could be demarcated on the plate on which *P. aeruginosa* PAO1 was grown. In contrast, PDO300 colonies had merged, and streaks of bacteria were present, and discrete single colonies could hardly be defined. The surface of wildtype *P. aeruginosa* colonies (Figure 3A and 3C) appeared macroscopically rougher than the surface of PDO300 (Figure 3B and 3D), which looked smoother due to higher alginate levels. In summary, these pictures showed that alginate overproducing *P. aeruginosa* exhibited a more mucoid phenotype and that it was possible to macroscopically distinguish very low and strongly enhanced alginate production. However, this method does not offer the possibility of quantification or observations at the single cell level. Nevertheless, it still has great potential for the detection of high levels of alginate because it is very straightforward and a macroscopic difference between the strains can be observed with the naked eye.

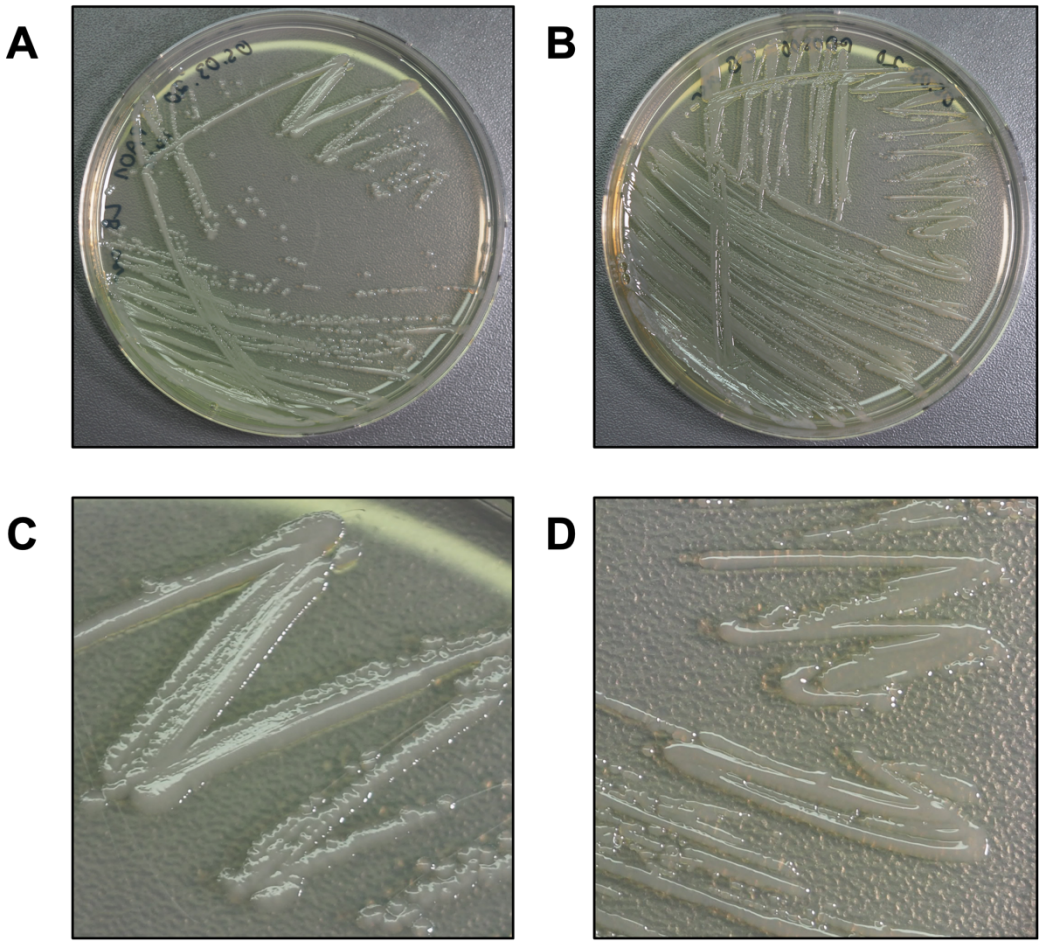

Figure 3: Colony morphology of P. aeruginosa PAO1 and P. aeruginosa PDO300 grown aerobically on LB agar plates
The P. aeruginosa wildtype PAO1 (A & C) produced distinct single colonies as well as large, merged colonies that formed streaks with a rough surface. In contrast, the alginate overproducing, mucoid strain P. aeruginosa PDO300 (B & D) produced almost no single colonies (B) but mainly merged colonies. Its surface was very smooth (D). This phenotypical difference is caused by alginate overproduction, i.e., mucoidy.

Furthermore, to test if O_2-deprivation leads to increased alginate levels in *P. aeruginosa* PAO1 sufficiently high to be observed macroscopically, PAO1 wildtype was grown on modified M9 plates supplemented with KNO_3 for anaerobic respiration. M9 is a minimal medium that was used to enhance alginate production and features the necessary substances that enable anaerobic growth. *P. aeruginosa* PAO1 was grown on M9 plates under aerobic and anaerobic conditions for 48 h. The PAO1 colonies showed a rough surface and many discrete colonies under aerobic conditions (Figure 4A). There were some in areas with densely grouped colonies, discrete colonies were partially detectable due to a discrete surface structure. However, presumably due to increased production of alginate after 48 h of anaerobic growth, the surface of PAO1 colonies was

different and appeared smoother compared with aerobic conditions (Figure 4B). Hardly any individual discrete colonies or even merged colonies could be observed, and streaks of bacteria rather than colonies were common. In contrast, individual colonies of PAO1 grown aerobically, as well as merged colonies could easily be identified. Notably, both bacterial cultures were incubated for the same time, but as bacteria grow slower under anaerobic conditions, the difference between the colony morphologies might have been more pronounced if the anaerobic cultures were incubated longer. In conclusion, these results suggest that an increase in alginate levels induced by O_2 deprivation can be observed macroscopically if the bacteria were grown for an extended period of time. However, this macroscopic analysis does not allow for the detection of immediate changes in alginate levels, due to the long incubation periods.

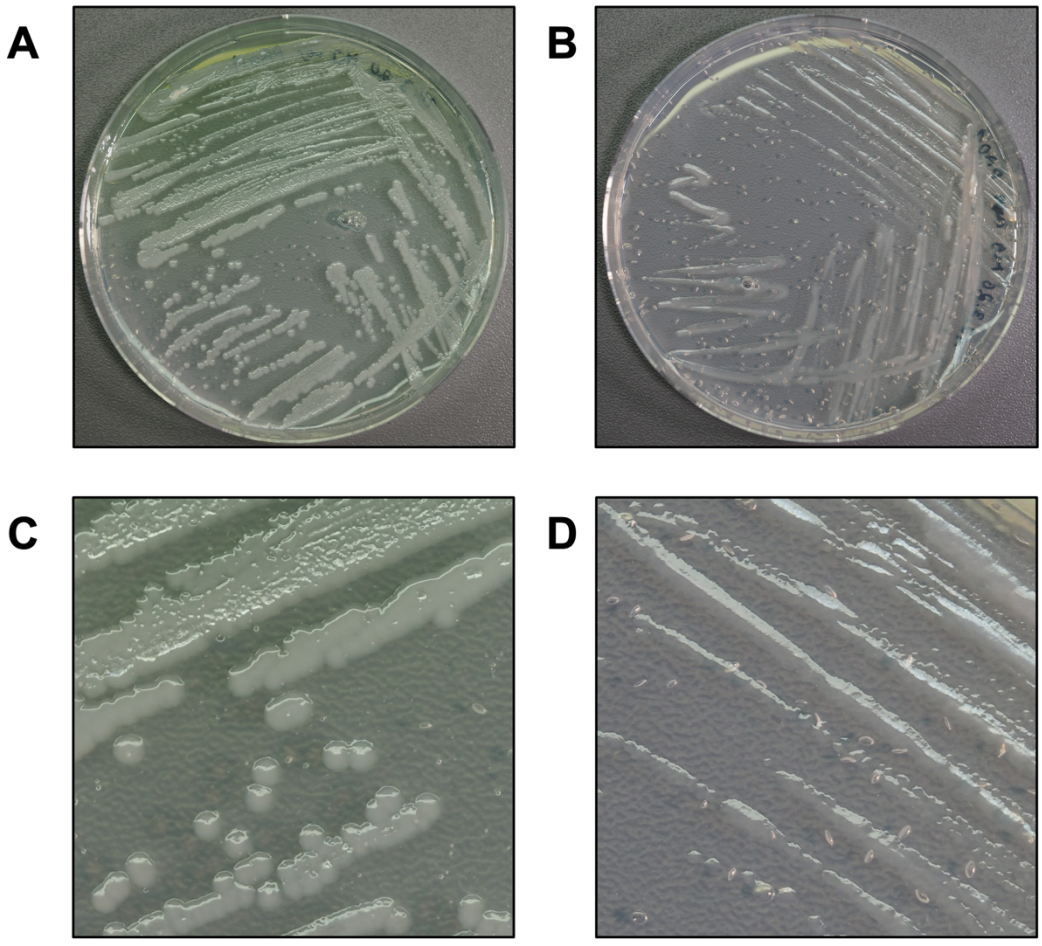

Figure 4: P. aeruginosa PAO1 incubated under aerobic and anaerobic conditions on M9 agar plates for 48 hours
Aerobically grown P. aeruginosa PAO1 exhibited many discrete single colonies and several streaks of colonies with a rough surface (A & C). The single colonies could still be demarcated (C). Colonies of P. aeruginosa PAO1 grown under anaerobic conditions showed a smoother appearance with fewer discrete colonies, indicating alginate synthesis (B & D).

3.2 Crystal violet staining of *P. aeruginosa*

3.2.1 Standard curves for the crystal violet assay

Standard curves of alginate were prepared by first adding 1 M $CaCl_2$ to commercially available sodium alginate dissolved in water, washing the calcium-alginate complex, staining with crystal violet, washing again, and eluting the dye with acetic acid. The incubation times and washing steps were optimized. In the beginning, the Ca-alginate complex as well as the crystal violet-stained alginate were washed with water and the samples were measured individually in cuvettes with a photometer. A centrifugation speed of 2500 rpm was chosen for washing the Ca-alginate, 3000 rpm were utilized for the crystal violet-stained alginate. The aim was to obtain a standard curve of the absorbance of crystal violet-stained alginate at different concentrations ideally displaying a linear relationship. The results of this first experimental set-up are depicted in Figure 5, showing the average values of three independent experiments, each performed with one replicate. The samples were diluted 1:1000 or 1:500. The absorbances of the samples of the concentrations between 0.2 and 1.0 mg/ml suggested a linear relationship because of low standard deviations. However, the values of the concentrations higher than 1.0 mg/ml show a high standard deviation, which suggested high variation in the data between experiments.

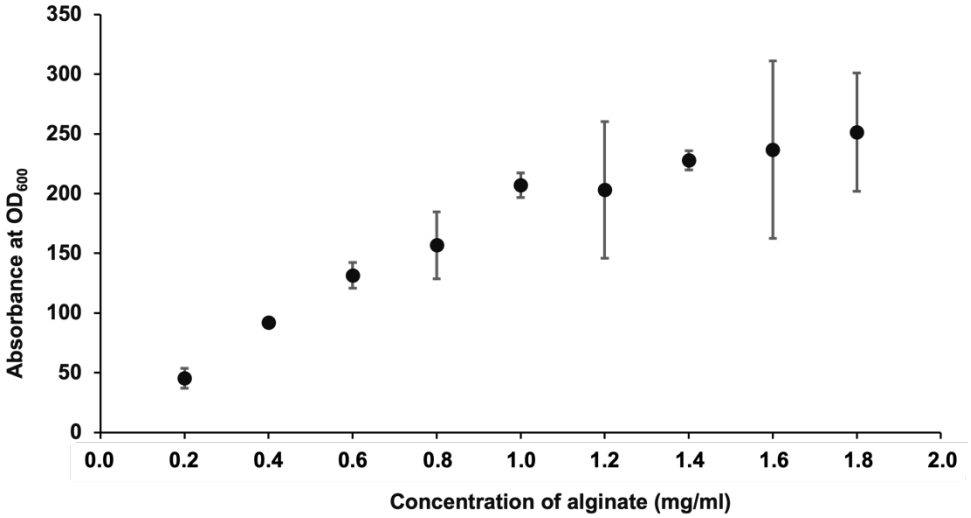

Figure 5: Standard curve of sodium alginate diluted in water and stained with crystal violet
Crystal violet staining of commercial alginate followed by elution by acetic acid and measurement of OD_{600} is shown. The x-axis shows the concentration of sodium alginate in mg/ml, whereas the y-axis shows the absorbance of the samples. The alginate concentration ranged from 0.2 to 2 mg/ml. Shown are the mean values of three independent experiments and the standard deviation. The latter ranged between 61 at 1.6 mg/ml and 2 at 0.4 mg/ml and was higher overall at higher concentrations.

From then on, the samples were measured with a plate reader using 96-well plates to improve efficiency. Notably the values from this procedure were lower and could not be compared to the measurements using a cuvette, due to a shorter optical path of the wells than the one of the cuvettes. In addition, the stained alginate was washed with 1% acetic acid for efficient removal of the excess crystal violet dye. LB without alginate was used as a negative control in order to obtain a zero-point of the standard curve, and to improve the accuracy of measuring alginate of *P. aeruginosa* cultures, in particular those with low alginate production. Next, standard curves were conducted using sodium alginate dissolved in LB medium instead of H_2O, because the bacteria would be cultured in LB medium. Figure 6 shows the results of three independent experiments, conducted under standard conditions. The individual experiments are depicted, the mean values with the standard deviation are depicted at Figure 7.

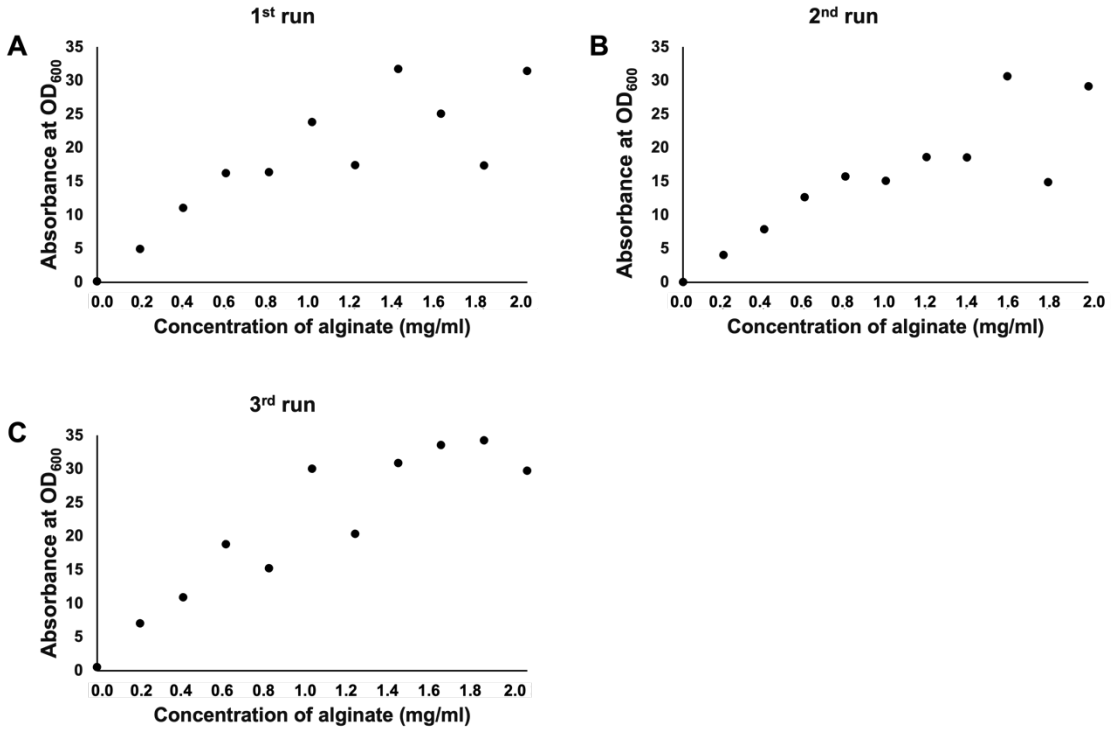

Figure 6: Standard curve of sodium alginate diluted in LB medium and stained with crystal violet
Crystal violet staining of commercial alginate followed by elution by acetic acid and measurement of OD_{600} is shown. On all the three graphs, the x-axis shows the concentration of alginate in mg/ml, which ranges between 0.0 and 2.0. The y-axis shows the absorbance, which ranges between 0.1 and 34.2. Throughout the three experiments, the absorbance at 0.0 mg/ml to 0.6 mg/ml suggested a linear relationship, deviating at higher concentrations. The results of three independent experiments are depicted.

In Figure 6A, the absorbance showed high variation at concentrations from 0.8 to 2.0 mg/ml, rather contradicting a linear relationship. In Figure 6B, most measuring points implied a linear relationship, except for 1.6 mg/ml and 1.8 mg/ml. Lastly, Figure 6C showed high variation at 0.8 to 1.2 mg/ml and 2.0 mg/ml, apart from that also corresponding to a linear relationship.

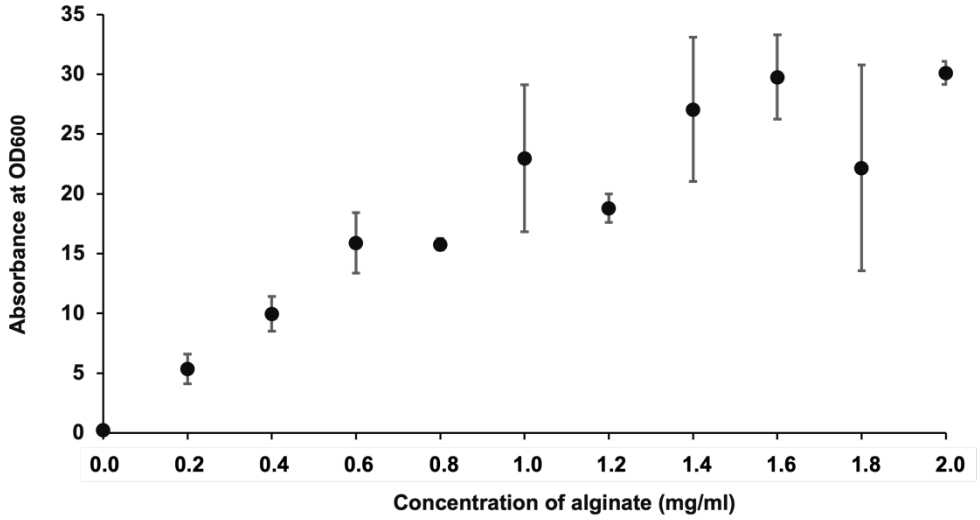

Figure 7: Standard curve of alginate diluted in LB medium and stained with crystal violet
Crystal violet staining of commercial alginate followed by elution by acetic acid and measurement of OD_{600} is shown. The average absorbance of three independent experiments, which are depicted in detail at Figure 6, as well as the standard deviation are depicted. The x-axis shows the concentration of alginate in mg/ml, which ranges between 0.0 and 2.0. The y-axis shows the absorbance, which ranges between 0.2 and 30.1.

The absorbance of the samples increased with the alginate concentration, from 5.35 at 0.2 mg/ml alginate to 30.11 at 2.0 mg/ml alginate. However, a high variation of the alginate concentrations from 1.0 mg/ml and a corresponding high standard deviation was observed (Figure 6 and 7). The standard deviation was between 0.21 at 0.0 mg/ml alginate and 8.60 at 1.8 mg/ml alginate. At the measuring points from 0.0 to 0.8 mg/ml alginate, the absorbance varied less, and the standard deviation was between 0.21 at 0.0 mg/ml alginate and 2.52 at 0.6 mg/ml alginate. Selected values could therefore correspond to a linear relationship, which will be analyzed in the following chapter.

3.2.2 Statistical analysis of the standard curves

Crystal violet staining of sodium alginate at known concentrations was conducted in order to obtain a standard curve to determine unknown concentrations of alginate produced by *P. aeruginosa*. The statistical analysis was performed by Dr. Ulrich Schoppmeier, Institute of Medical Microbiology and Hygiene, University Hospital Tübingen, with the statistical software R (Appendix 1). The data of three independent experiments (Figure 6 and 7) were plotted in a diagram (Figure 8).

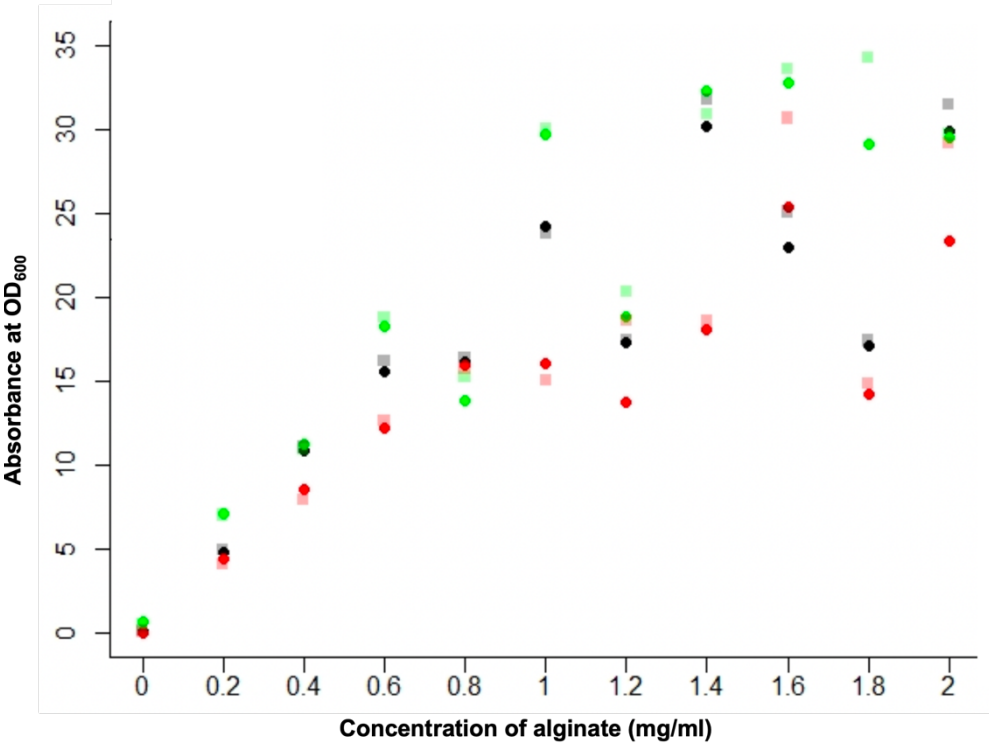

Figure 8: Standard curves obtained from three independent experiments of alginate diluted in LB medium and stained with crystal violet
Crystal violet staining of commercial alginate followed by elution by acetic acid and measurement of OD_{600} is shown. The x-axis shows the concentration of alginate, the y-axis the absorbance. Three independent experiments were performed, at the end of the experiment the eluate of the stained alginate was diluted 1:10 and 1:20. Different independent experiments are indicated by colors (red, green, black). Each concentration of each independent experiment is depicted by two data points that refer to the different dilutions of the eluate at the end of the experiment (circle: 1:10; square: 1:20).

There is low variation of the values measured for alginate concentrations ranging from 0.0 mg/ml to 0.8 mg/ml. The obtained values indicate a linear relationship. At the measuring points from 1.0 to 2.0 mg/ml, high variation between the different experiments was observed. However, the variation between the different dilutions is low, which suggests that the high variation is not caused by the dilution of the samples at the end of the experiment. Different polynomial functions were fitted to the data, among which a polynomial function of second degree was found to be the most adequate (see 2.8.3). The coefficients, results and p-values are displayed in the appendix at Table 7.

Figure 9 shows this function as well as prediction bands of the three standard curves (see Figure 6) of alginate stained with crystal violet. Prediction bands indicate where the data of further experiments would be expected if the

experiment was run many times. As 95% prediction bands were calculated, 95% of the data would be expected within the prediction bands. This expectation conforms to the results, as only two data points are located outside of the prediction bands. However, the prediction bands are very large, which suggests that the data points would be located in a large range, if the experiment would be run many times. Therefore, this function would not reliable enough to be used for the calculation of alginate concentrations.

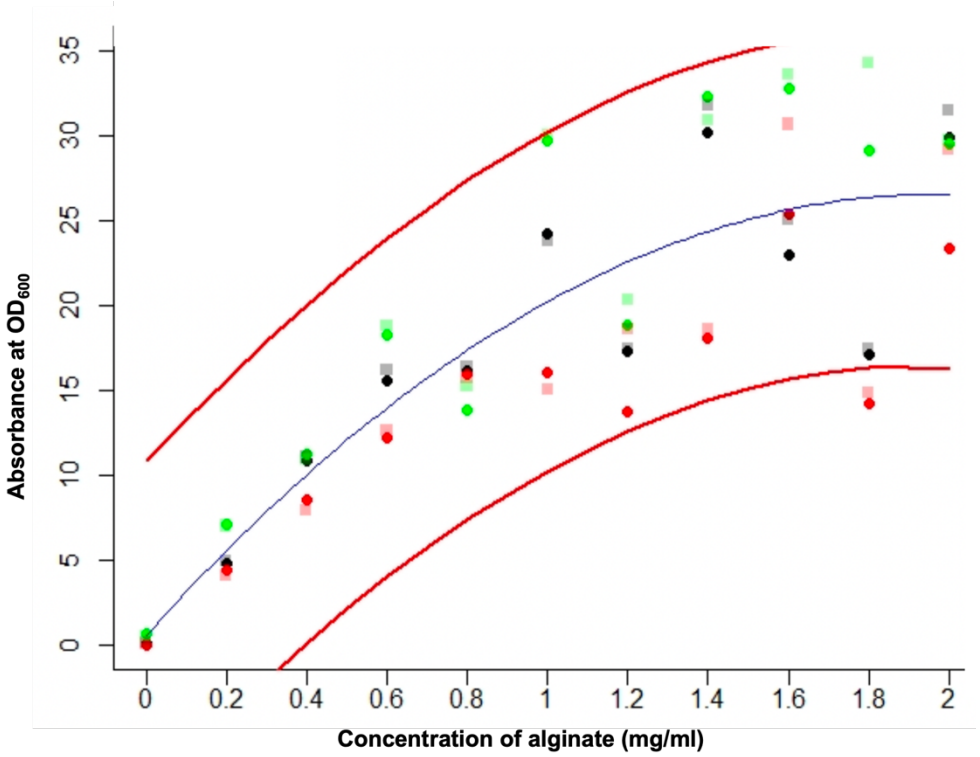

Figure 9: Prediction bands of standard curves obtained from three independent experiments of alginate diluted in LB medium and stained with crystal violet
Crystal violet staining of commercial alginate followed by elution by acetic acid and measurement of OD_{600} is shown. The y-axis shows the absorbance, the x-axis the alginate concentration in mg/ml. The dots indicate the results of the experiments, the red lines the graphs of the prediction bands. Those bands indicate where 95% of the data of further experiments would be expected, if the experiment was run many times. The blue line is a polynomial function of second degree that was fitted to the data. For these experiments, the crystal violet was eluted with acetic acid, diluted 1:10 and 1:20.

As the absorbance of the lower alginate concentrations varied less between experiments, a linear regression was fitted to the data, which would be more practical for the calculation of unknown concentrations (see 2.8.3). The coefficients, results, and t-values are displayed in the appendix in Table 8. Figure 10 shows the linear regression of concentrations between 0.0 and 0.8 mg/ml with

confidence and prediction bands. The confidence bands indicate where 95 % of the regression lines would be, if the experiment was run many times. Compared to Figure 9, the prediction bands are much narrower. This suggests that the linear regression (of the alginate concentrations between 0.0 and 0.8 mg/ml) would be more reliable than the polynomial of second degree (of the alginate concentrations between 0.0 and 2.0 mg/ml). However, the prediction bands are still large. If, for example, an absorbance of 5 was measured, the concentration of alginate could be anywhere between 0.0 and 0.4 mg/ml. This means that the linear regression would still not be adequate for detecting small changes in alginate levels.

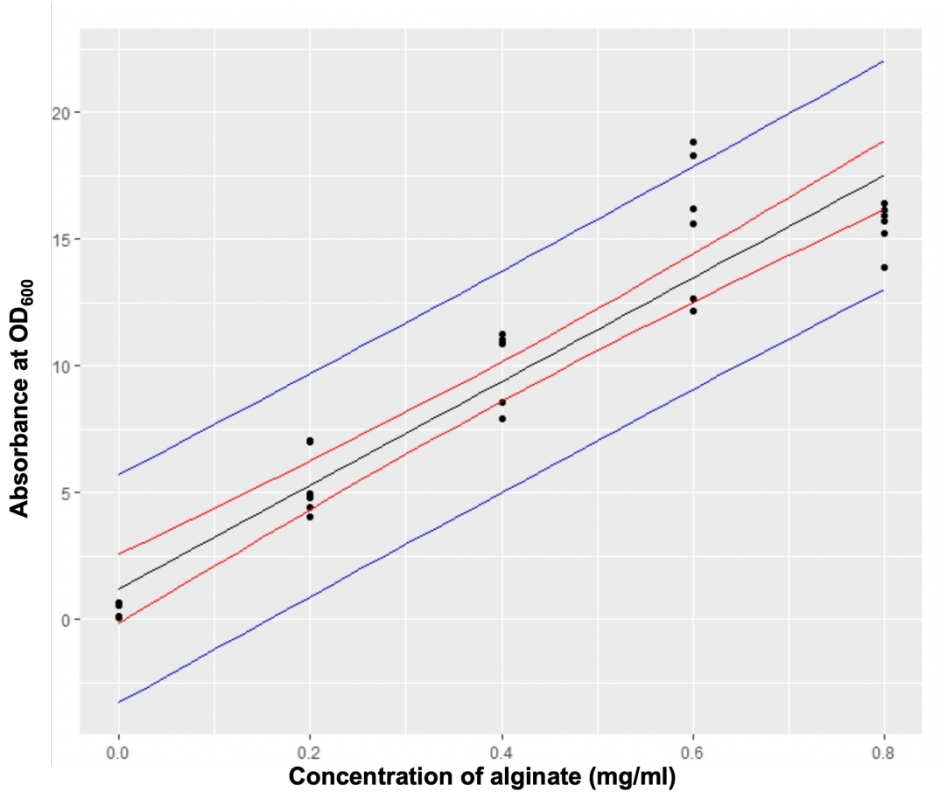

Figure 10: Linear regression of standard curves obtained from three independent experiments of alginate diluted in LB medium and stained with crystal violet.
Crystal violet staining of commercial alginate followed by elution by acetic acid and measurement of OD_{600} is shown. The x-axis shows the concentration of alginate, the y-axis the absorbance. The black line indicates a fitted regression line, the red lines 95% confidence bands and the blue lines 95% prediction bands. The prediction bands shows where 95% of the data, i.e. the measured absorbance of dyed alginate, would be expected when further sample points would be taken. The confidence bands, indicate the location of the regression lines, if the experiment was run many times. Concentrations from 0.0 to 0.8 mg/ml are depicted.

3.2.3 Crystal violet staining of non-mucoid and mucoid P. aeruginosa culture supernatants

Alginate levels were determined of *P. aeruginosa* grown in LB broth under aerobic conditions. The bacteria were cultivated in LB medium, centrifuged, and the supernatant was then processed for staining of alginate with crystal violet (see 2.8.2). As a first approach, it was tested if the crystal violet staining method was suitable for differentiating between no and high alginate production by *P. aeruginosa*. *P. aeruginosa* wildtype PAO1 and the alginate overproducing strain *P. aeruginosa* PDO300 were selected as strains for the following experiments. As *P. aeruginosa* PAO1 does not produce alginate under the aerobic conditions and *P. aeruginosa* PDO300 overproduces alginate, the absorbance of the crystal violet eluate of *P. aeruginosa* PDO300 was expected to be considerably higher compared to *P. aeruginosa* PAO1. $CaCl_2$ was added to the supernatant of *P. aeruginosa* PAO1 and *P. aeruginosa* PDO300 liquid cultures, which produced aggregation in some experiments in both strains in the form of clumping and increased viscosity. At this time, the cultures were standardized to an OD of 0.05 at the beginning of the incubation period. In the initial experiments, *P. aeruginosa* PAO1 and *P. aeruginosa* PDO300 were grown in LB for the same amount of time and alginate was stained with crystal violet according to the protocol described in 2.8.2. Different dilutions of the crystal violet eluted from precipitated alginate were prepared. Overall, there was little variation between the different dilutions, except for the 1:1000 dilution, which was therefore omitted in further experiments in favor of a dilution of 1:10 and 1:20.

The OD_{600} of the bacterial cultures was measured directly before processing the samples. For the experiment depicted in Figure 11, the culture OD_{600} was 0.357 for *P. aeruginosa* PAO1 and 0.288 for *P. aeruginosa* PDO300 at the time of harvesting. The supernatant of each culture was split in half and processed as technical replicates of 20 ml each to evaluate the variability. In accordance with the higher alginate production of PDO300, the absorbance of the *P. aeruginosa* PDO300 crystal violet eluate was higher than the absorbance of the *P. aeruginosa* PAO1 crystal violet eluate for both technical replicates (Figure 11). However, the OD_{600} of the PAO1 crystal violet eluate was considerably higher

than zero. This was not expected, as *P. aeruginosa* PAO1 does not produce alginate under aerobic conditions. It is possible that a small quantity of crystal violet was retained in the alginate and could not be washed out. Another reason could be background noise because of other calcium-binding components that were present in the supernatant of PAO1. To further explore this result, more replicates of this method were performed.

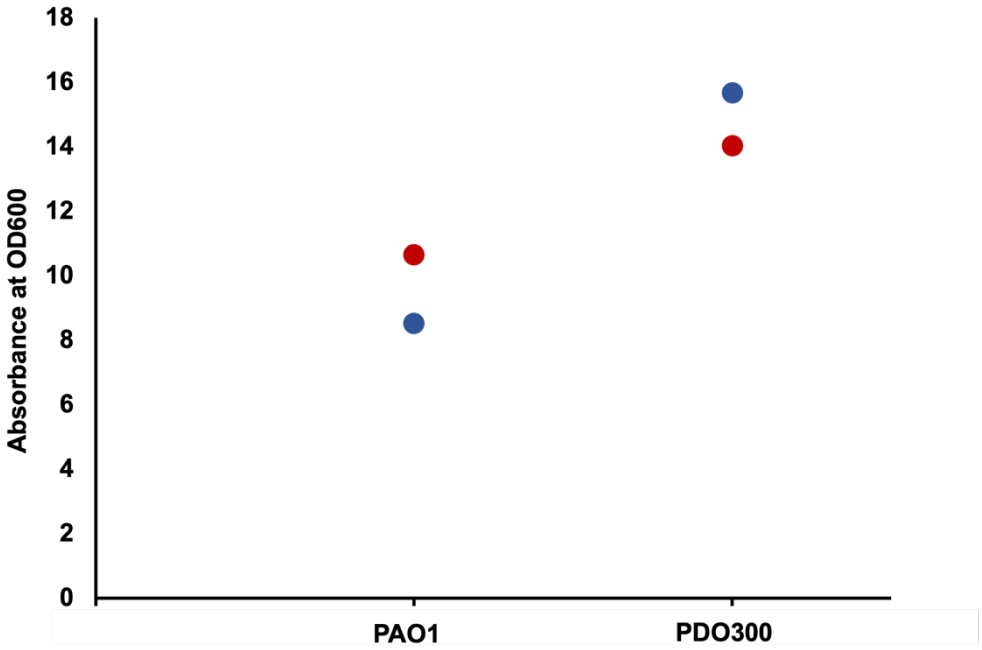

Figure 11: Crystal violet staining of precipitated alginate of culture supernatants of P. aeruginosa PAO1 and PDO300
Crystal violet staining of P. aeruginosa cultures followed by elution by acetic acid and measurement of OD_{600} is shown. The x-axis shows the wildtype P. aeruginosa PAO1 and the alginate overproducing mutant P. aeruginosa PDO300; the y-axis shows the average absorbance of the crystal violet eluate from precipitated, and dyed alginate. The red and blue dots indicate two different batches: The bacterial cultures were split half and then treated as technical replicates. Overall, the absorbance corresponding P. aeruginosa PDO300 (14-15.7) is higher than the one corresponding to P. aeruginosa PAO1 (8.5-10.7).

To further improve the experimental procedure, the PAO1 and PDO300 cultures were harvested at the same OD_{600}. After 24 h, the OD_{600} of both cultures was measured and the culture with the lower OD_{600} was kept in an incubator at 37°C until the OD_{600} was the same. Figure 12 shows the results of nine independent crystal violet staining assays conducted under the same circumstances. The same colors refer to the same experiments. In all experiments except one (indicated by the red dot), the absorbance of *P. aeruginosa* PDO300 was higher than the absorbance of PAO1. The mean absorbance of PAO1 was at 5.3, while the mean absorbance of PDO300 was at 7.6. However, the inter-experimental

variation was very high, with the absorbance of *P. aeruginosa* PAO1 ranging between 0.5 and 11.4 and the absorbance of *P. aeruginosa* PDO300 ranging between 1.2 and 11.8. The results show that even high alginate production cannot be reliably measured by crystal violet staining.

As mentioned above, two tubes per strain per experiment were processed. One tube was treated according to the standard protocol, for the other, different conditions were tested in order to improve the protocol. The following conditions were tested: More washing steps or increased centrifugation speed of the unstained Ca-alginate to eliminate a high background signal responsible for the high absorbance of the PAO1 alginate crystal violet sample. Furthermore, the addition of 4 ml crystal violet instead of 2 ml was tested to eliminate the possibility that the PDO300 alginate sample was not fully saturated with crystal violet. These attempts to optimize the assay did not improve the outcome and did not reduce the variability of the results.

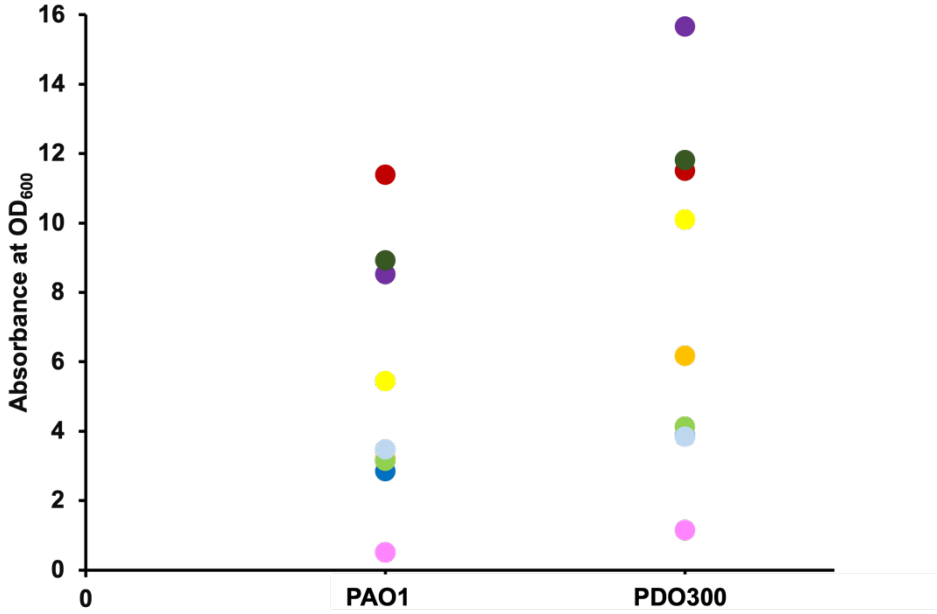

Figure 12: Results of nine independent experiments of P. aeruginosa crystal violet staining conducted under standard conditions
Crystal violet staining of P. aeruginosa cultures followed by elution by acetic acid and measurement of OD_{600} is shown. Nine independent experiments conducted under standard conditions are depicted. The x-axis shows the wildtype P. aeruginosa PAO1 and the alginate overproducing mutant P. aeruginosa PDO300; the y-axis shows the absorbance of the eluate from precipitated and crystal violet-stained alginate. The same colors refer to same experiments. Overall, the absorbance of P. aeruginosa PDO300 was higher than the absorbance of P. aeruginosa PAO1, but the inter-experimental variation was very high.

3.2.4 Crystal violet staining of P. aeruginosa PAO1, PDO300 and sadC mutants

Furthermore, to test if the crystal violet assay is suitable for the detection of intermediate differences in alginate levels caused by low oxygen tensions in non-mucoid *P. aeruginosa*, crystal violet staining of two other *P. aeruginosa* strains was tested. *P. aeruginosa* PAO1Δ*sadC* contains an unmarked in-frame deletion of the *sadC* gene which was tested in order to determine the alginate content after removing *sadC*. In *P. aeruginosa* PAO1*sadC*ΔTM only the transmembrane domain of *sadC* is missing, but the cytoplasmic domain containing the GGDEF motif is expressed. This strain was examined to determine the remaining alginate expression and therefore identify the role of the transmembrane domain of *sadC* in alginate production. *SadC* is a diguanylate cyclase that is required for immediate and intermediate increase of alginate production under anaerobic conditions (see 1.5). Figure 13 shows two independent crystal violet staining experiments using *P. aeruginosa* PAO1*sadC*ΔTM, PAO1Δ*sadC* as well as *P. aeruginosa* PAO1 (grown aerobically and anaerobically) and *P. aeruginosa* PDO300. For PAO1, only one experiment was performed. The cultures were not normalized to OD_{600}.

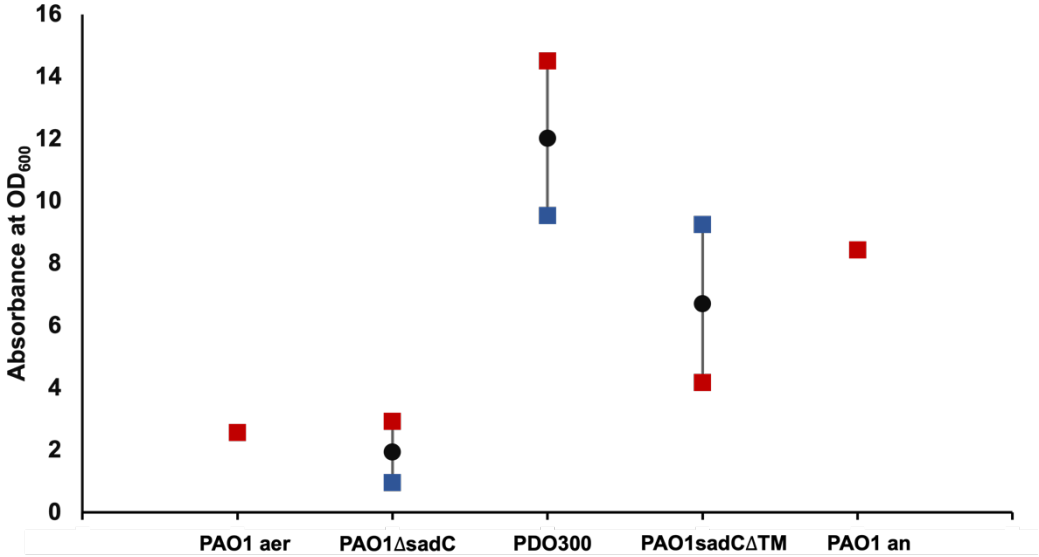

Figure 13: Crystal violet staining of P. aeruginosa PAO1, PDO300, PAO1sadCΔTM and PAO1ΔsadC
Crystal violet staining of P. aeruginosa cultures followed by elution by acetic acid and measurement of OD_{600} is shown. The diagram shows the data of two independent experiments, and their mean values. The x-axes show the different strains of P. aeruginosa that were tested: Aerobically grown P. aeruginosa PAO1, than P. aeruginosa PAO1ΔsadC, which is aerobically grown P. aeruginosa PAO1 with an unmarked in-frame deletion of sadC and the aerobically grown alginate overproducing mutant P. aeruginosa PDO300. PAO1sadCΔTM is aerobically grown P. aeruginosa PAO1 with a deletion of only the transmembrane domain of sadC, the cytoplasmic domain containing the GGDEF motif still being expressed. PAO1 an is anaerobically grown P. aeruginosa PAO1 wild type. The y-axis shows the average absorbances of the crystal violet eluate from precipitated, and stained alginate.

The absorbance was lowest for aerobically grown *P. aeruginosa* PAO1 and *P. aeruginosa* PAO1Δ*sadC*, while it was higher for *P. aeruginosa* PAO1*sadC*Δ*TM* and anaerobically grown *P. aeruginosa* PAO1 and highest for *P. aeruginosa* PDO300. *P. aeruginosa* PDO300 is an alginate overproducing mutant, which corresponds to the high absorbance of this strain upon crystal violet staining (Figure 13). Both PAO1Δ*sadC* and the wildtype do not produce alginate under aerobic conditions, which corresponds to their low and similar absorbance (Figure 13). The absorbance of PAO1*sadC*ΔTM was intermediate, which is most likely due to measurement inaccuracy in the sense of a false-high value (Figure 13). *P. aeruginosa* PAO1 does not produce alginate under aerobic conditions, which explains the low absorbance of aerobically grown PAO1 in the crystal violet assay (Figure 13). The results of *P. aeruginosa* PDO300 and PAO1*sadC*ΔTM show a high standard deviation, corresponding to the high variation in previous experiments. The standard deviation of *P. aeruginosa* PAO1 is moderate. These experiments show less variation than previous experiments. Nevertheless, in

view of the other results, the crystal violet assay is not suitable for measuring small changes in alginate levels, due to the high variation of the results.

3.3 Alcian blue staining of *P. aeruginosa*

Alcian blue (AB) is a basic dye that is usually used in histology to stain acidic substances such as mucins. Since alginate is negatively charged the dye could potentially be used to visualize it on bacterial cells using microscopy. However, to the best of our knowledge, Alcian blue has not been used so far for staining alginate. Thus, the aim was to probe whether this technique is suitable to detect alginate at the single cell level.

P. aeruginosa PAO1 and *P. aeruginosa* PDO300 were grown on LB plates and harvested after three days of incubation at 37°C. The bacteria were suspended in sterile H_2O, streaked out on glass slides and heat fixed. The slides were stained with 1:10 diluted Alcian blue for 1 min and then washed with H_2O. They were imaged using a 100x objective. In Figure 14, a difference between the two strains was observed. Overall, the staining was more intense for the alginate overproducing mutant *P. aeruginosa* PDO300. In Figure 14B, representing *P. aeruginosa* PDO300*,* blue streaks visible between the single bacteria are likely representing alginate. However, it is theoretically possible that the blue streaks represent another substance present in the bacterial culture, such as other polysaccharides, DNA fragments or lyzed cells (Franklin et al., 2011). PAO1 on the contrary showed no streaks, and the background was a paler color, which might indicate the lack of alginate (Figure 14A). In Figure 14B PDO300 seems slightly bluer and more globular than the wildtype. Areas surrounding the PDO300 bacteria were also stained blue potentially indicating the presence of alginate.

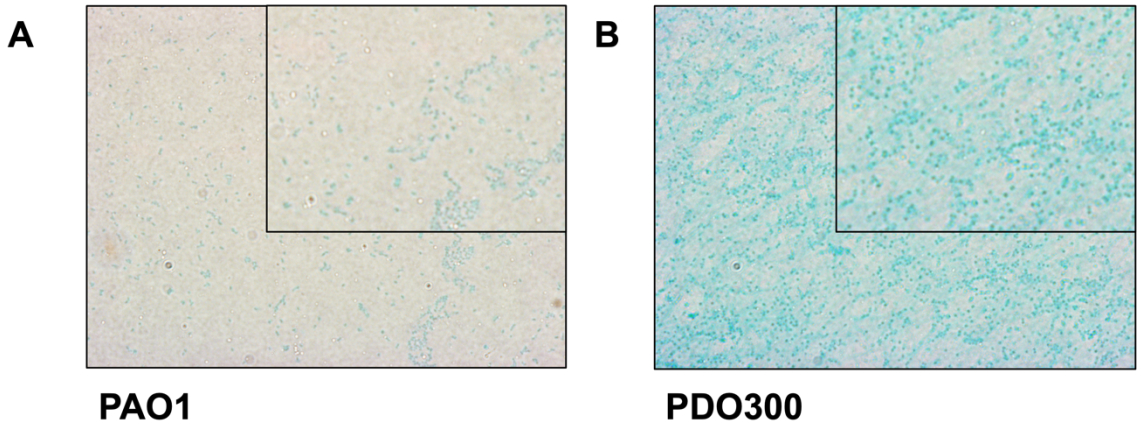

Figure 14: Alcian blue staining of P. aeruginosa PAO1 and PDO300 after growth on LB agar plates for 3 d
The P. aeruginosa wildtype PAO1 (A) and alginate overproducing mutant P. aeruginosa PDO300 (B) were shown in 100x magnification. The strains were cultivated on LB plates for 3 d and stained with 1:10 diluted Alcian blue. On both images, several bacteria were visible. P. aeruginosa PAO1 appeared more rod-shaped while P. aeruginosa PDO300 showed a rounder form. While PAO1 featured a light background (A), blue streaks appeared between the PDO300 bacteria (B).

In order to reduce background staining to improve the visualization of individual bacterial cells and after Alcian blue staining of *P. aeruginosa* 1 d LB plate cultures were used and the bacteria were washed before the staining with H_2O. The bacteria were then spread on a glass slide, dried, heat fixed, stained with Alcian blue and washed one time with H_2O. This led to a decrease of background noise. Around several individual bacterial cells and groups of bacteria of *P. aeruginosa* PDO300, blue halos were observed, likely indicating alginate secreted by the bacteria (Figure 15B). In contrast, these halos were absent from PAO1 (Figure 15A). However, there were still *P. aeruginosa* PDO300 bacteria present that did not express this effect to the same extent (Figure 15). To explore if this staining is suitable, the reproducibility was tested.

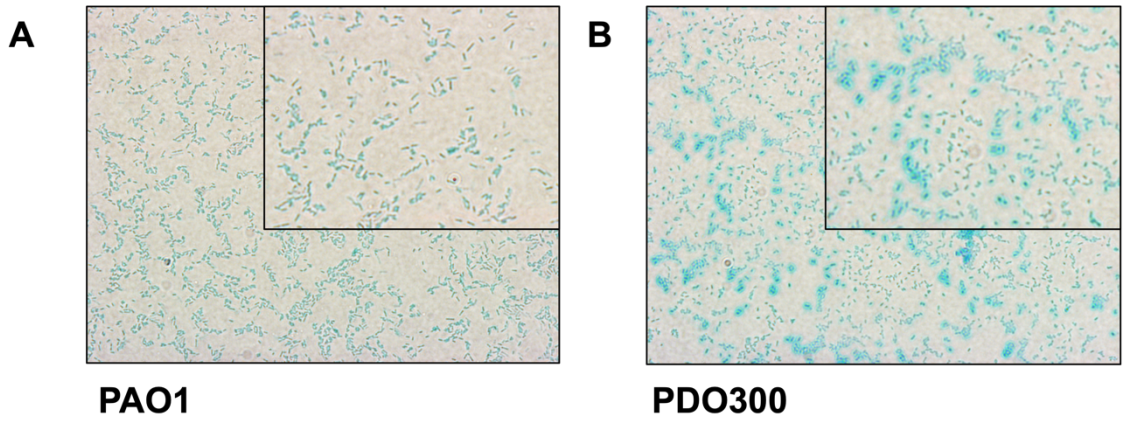

Figure 15: Alcian blue staining of P. aeruginosa PAO1 and P. aeruginosa PDO300 grown on LB agar plates, washed with H_2O
The P. aeruginosa wildtype PAO1 (A) and alginate overproducing mutant P. aeruginosa PDO300 (B) are shown in 100x magnification. The strains were cultivated on LB plates for 1 d and stained with 1:10 diluted Alcian blue. Blue bacteria are visible on both images, with a similar, pale background. The P. aeruginosa PAO1 bacteria are tinted a little lighter and more rod-shaped (A) than the P. aeruginosa PDO300 bacteria (B). The P. aeruginosa PDO300 bacteria have a darker color and more circular shape (B). Around several P. aeruginosa PDO300 bacteria, the background is colored blue, surrounding the bacteria like halos (B).

Using this procedure, it was difficult to differentiate between the bacterial cells and the alginate surrounding the bacteria. The original experiment was then replicated in order to test reproducibility. As shown in Figure 16, the two strains looked very similar, except for a rounder shape and a little difference in color of *P. aeruginosa* PDO300, no obvious difference could be observed. As a sufficient microscopically detectable difference of the two strains could not be reproduced anymore, a new approach of fixation was tested. It was suspected that the hydrated alginate matrix surrounding the bacterial cell was damaged, i.e. dehydrated by heat fixation. To eliminate this interference, the bacteria were fixed with the crosslinker 4% formaldehyde (FA) to preserve the hydrate envelope.

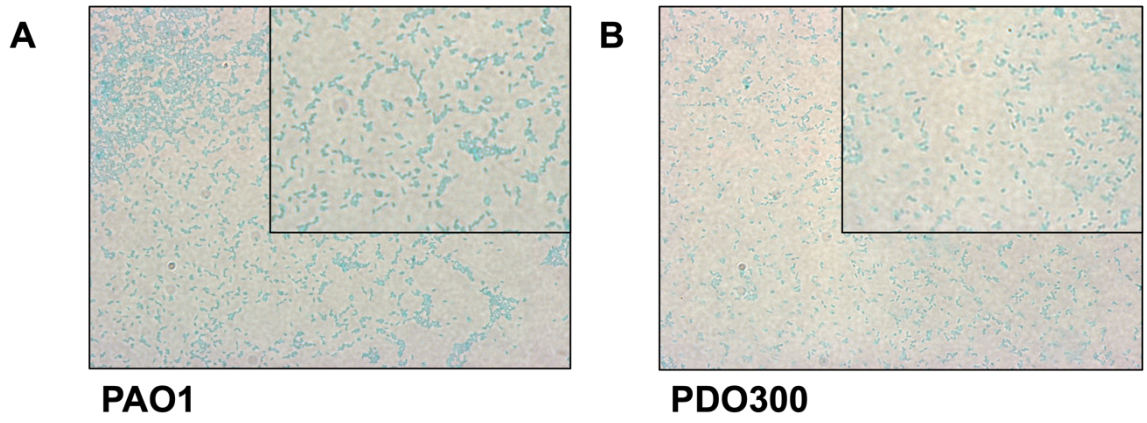

Figure 16: Alcian blue staining of P. aeruginosa PAO1 and P. aeruginosa PDO300 grown on LB agar plates, washed with H_2O
The P. aeruginosa wildtype PAO1 (A) and alginate overproducing mutant P. aeruginosa PDO300 (B) are shown in 100x magnification. The strains were cultivated on LB plates for 2 d, stained with 1:10 diluted Alcian blue. On a pale background, blue-tinted bacteria were visible on both images. Apart from a slightly more globular shape and a darker color of some bacteria of P. aeruginosa PDO300, there was no visible difference between the strains.

Figure 17 shows Alcian blue staining of *P. aeruginosa* PAO1 and PDO300 grown on LB plates, fixed with 4% formaldehyde and stained with Alcian blue. Several differences in the appearance of the two strains were visible: The blue halos appeared again, and blue streaks were visible in the background of *P. aeruginosa* PDO300. These findings indicate a staining of alginate by Alcian blue. Fixation by 4% FA was hence implemented in the protocol, as it improved the quality of the alginate staining.

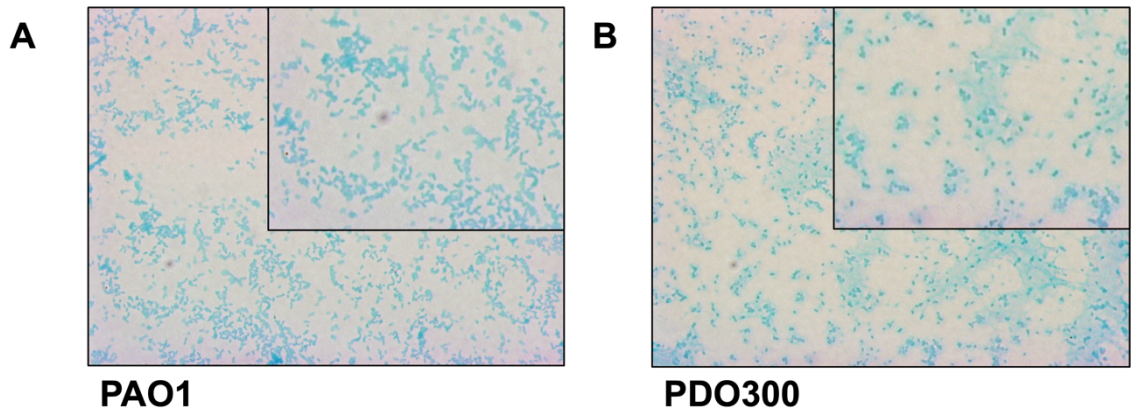

Figure 17: Alcian blue staining of P. aeruginosa PAO1 and P. aeruginosa PDO300, 4% FA fixation
The P. aeruginosa wildtype PAO1 (A) and alginate overproducing mutant P. aeruginosa PDO300 (B) are shown in 100x magnification. The strains were cultivated on LB plates for 4 d, stained with 1:10 diluted Alcian blue, fixed with 4% FA on glass slides. While the background of the wildtype was pale and unicolor (A), blue streaks could be observed in the near environment of P. aeruginosa PDO300 (B). The P. aeruginosa PDO300 bacteria appeared darker in color and sometimes show blue halos.

This experiment was repeated in order to test reproducibility.

Figure 18 shows *P. aeruginosa* PAO1 and *P. aeruginosa* PDO300 grown on LB plates for 3 d, streaked out on glass slides, stained with Alcian blue and fixed with 4% FA. *P. aeruginosa* PAO1 is depicted in Figure 18A and *P. aeruginosa* PDO300 on Figure 18B. Once again, blue halos were detected around the *P. aeruginosa* PDO300 bacteria, and blue streaks were visible in the background, but the effect was weaker than in earlier experiments (see Figure 15 and 18).

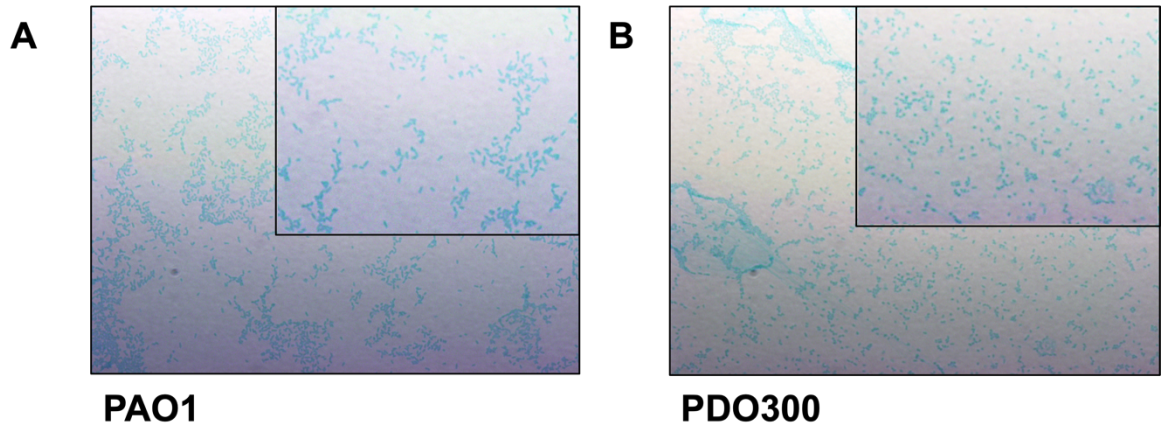

Figure 18: Alcian blue staining of P. aeruginosa PAO1 and P. aeruginosa PDO300 after 4% FA fixation
The P. aeruginosa wildtype PAO1 (A) and alginate overproducing mutant P. aeruginosa PDO300 (B) are shown in 100x magnification. The strains were cultivated on LB plates for 3 d, fixed with 4% FA on coverslips and washed with PBS buffer. They were stained with 1:10 diluted Alcian blue and washed with sterile H_2O. Bacteria of a similar blue color were visible on both slides, the P. aeruginosa PDO300 strains showed slight halos and light blue streaks between the bacteria (B). In this and some other experiments, the bacteria formed distinctive crystal-like shapes on the slides and showed clumping (A & B). This occurred in both strains and is therefore probably unrelated to alginate production and could be caused by PBS buffer.

Advantages of the Alcian blue staining assay include its very simple, straightforward approach and that it does not require special equipment or hazardous chemicals. It showed promising results, enabling the differentiation between *P. aeruginosa* wildtype and an alginate overproducing mutant, and the opportunity of analyzing the bacteria on the single cell level. However, due to the high variation in the results the Alcian blue assay is currently not optimal for the detection of alginate produced by *P. aeruginosa.*

4 Discussion

Methods for the quantification of polysaccharides have been used and developed for a very long time, the first version of the commonly used carbazole assay dates back as far as 1947 (Dische, 1947; Zheng et al., 2016). It was then modified and applied to alginate quantification by Knutson and Jeanes (Knutson & Jeanes, 1968). Alginate overproduction by *P. aeruginosa* occurs during the chronic stage of infection (Franklin et al., 2011). In *P. aeruginosa*, all alginate biosynthesis genes except for one are located in a single operon (Chitnis & Ohman, 1993; Ertesvåg et al., 2017). Expression of this gene cluster is controlled by several regulators. Mutations in regulatory genes can result in overexpression of the alginate biosynthesis gene cluster leading to a mucoid phenotype (Hassett et al., 2009; Hogardt & Heesemann, 2010; Wang, 2017). However, in addition to mutations, there is evidence that alginate production can be enhanced by non-mucoid *P. aeruginosa* within minutes due to regulatory events (Schmidt et al., 2016). Alginate production can be enhanced for example as an immediate response to low oxygen tensions, which is regulated post-translationally by the signaling molecule c-di-GMP produced by the diguanylate cyclase *sadC* (Schmidt et al., 2016). The level of this alginate production is intermediate and lower compared to the alginate production of mucoid *P. aeruginosa* isolates constitutively overexpressing the alginate biosynthesis gene cluster (Schmidt et al., 2016). To further investigate this pathway, it is necessary to find a sensitive and straightforward method for quantifying intermediate alginate concentrations. So far, an immunofluorescence assay has been used for this purpose (Garner et al., 1990; Schmidt et al., 2016). Due to variations in antiserum batches and alginate staining results, alternative techniques were tested in this work.

The aim of this work was to test different methods that are presumably applicable for smaller changes in alginate levels. In this work, cultivation on M9 agar plates, the quantitative crystal violet assay and the semiquantitative Alcian blue staining assay were tested. Whilst the crystal violet assay was first described by Zheng et

al., the Alcian blue staining for alginate visualization was tested for the first time (Zheng et al., 2016).

4.1 Colony morphology of *P. aeruginosa* cultured on different media

P. aeruginosa PAO1 and PDO300 were cultured aerobically on LB plates. While *P. aeruginosa* PAO1 showed discrete single colonies, *P. aeruginosa* PDO300 produced merged colonies with a smooth surface and a mucoid phenotype. This is consistent with the fact that PDO300 is a mutant of PAO1 expressing the *mucA22* allele, which results in the overexpression of the alginate operon and mucoidy (Mathee et al., 1999). Thus, alginate overproducing mutants can be distinguished in agar plate cultures from non-mucoid phenotypes with little to no alginate production. The cultivation of *P. aeruginosa* PAO1 aerobically and anaerobically on M9 minimal medium plates was tested as a new method. Anaerobically grown *P. aeruginosa* PAO1 produced smooth streaks of bacteria with no distinguishable single colonies, whereas aerobically grown *P. aeruginosa* PAO1 colonies exhibited a rougher surface with many distinct single colonies. As a mucoid phenotype is related with enhanced alginate production, it is suspected that *P. aeruginosa* PAO1 produced alginate under anaerobic conditions (Hogardt & Heesemann, 2010). Bragonzi et al determined the alginate levels produced by anaerobically grown *P. aeruginosa* PAO1 using the carbazole assay and indirect immunofluorescence (Bragonzi et al., 2005). They showed that alginate production of *P. aeruginosa* PAO1 was increased within 24 hours of anaerobic growth (Bragonzi et al., 2005), which corresponds to our findings. Cultivation of *P. aeruginosa* on M9 plates is an easy method of alginate detection that does not require special equipment or hazardous chemicals. However, this method does not offer the possibility of quantification and needs further verification by including a mutant that is unable to synthesize alginate. Still, being able to observe increased alginate production by an anaerobically grown non-mucoid isolate of *P. aeruginosa* with the naked eye, is a new finding and could lead the path to a new method of alginate detection.

4.2 Crystal violet staining as a quantitative method to measure alginate concentrations

The crystal violet assay is a newer method of alginate measurement that was first described by Zheng et al (Zheng et al., 2016). Alginate was precipitated with Ca^{2+} ions, which is possible because it is negatively charged (Page & Sadoff, 1975). The resulting Ca-alginate complex was stained with crystal violet (Zheng et al., 2016). Alginate from *P. aeruginosa* cultures was precipitated with $CaCl_2$, stained with crystal violet, the OD_{600} was measured, and the alginate concentration was determined using a standard curve of commercially available purified sodium alginate (Zheng et al., 2016). According to Zheng et al., the crystal violet assay was appropriate to measure alginate concentrations as low as 0.05 mg/ml, it did does not produce a background signal for LB medium and therefore did not require purification nor dilution of the alginate unlike the established carbazole assay (Zheng et al., 2016).

According to Zheng et al., after adding $CaCl_2$ to a sample of commercially available alginate or culture supernatant of *P. aeruginosa* PA2192, a mucoid isolate from a CF patient, a Ca-alginate aggregate formed (3.2) (Hanna et al., 2000; Zheng et al., 2016). No aggregate formed after adding $CaCl_2$ to LB medium or non-mucoid *P. aeruginosa* PAO1 (Zheng et al., 2016). This supports the notion that $CaCl_2$ can aggregate alginate. In this work, $CaCl_2$ was added to liquid cultures of wildtype *P. aeruginosa* PAO1 and the alginate overproducing mutant *P. aeruginosa* PDO300, but none of the strains showed aggregation, in contrast to the results of Zheng et al (see 3.2.3) (Zheng et al., 2016). It was suspected that the concentration of $CaCl_2$ was too low to aggregate the alginate in the bacterial cultures, so in order to saturate the alginate sufficiently with Ca^{2+}, a concentration of 1 M $CaCl_2$ was utilised in further experiments. In those experiments, aggregation of *P. aeruginosa* cultures upon addition of $CaCl_2$ could sometimes be observed, but not always. Furthermore, sometimes the wildtype showed aggregation as well, which could be due to an interfering substance in the sample that can bind to Ca^{2+}, which will be discussed later in this work.

In order to be able to determine the levels of alginate produced by *P. aeruginosa*, it was necessary to establish a standard curve using commercially available

sodium alginate. Several difficulties occurred when treating the alginate samples: It was aimed to preserve as much as possible of the Ca-alginate whilst still discarding enough of the supernatant to adequately wash the alginate, which was done by centrifugation. However, it was difficult to discard the supernatant, as the pellet was often very brittle and not solid enough. As a result, the pellet was sometimes poured out or aspirated with the supernatant, depending on the method of discarding the supernatant. This was especially relevant for the crystal violet-stained alginate, which often formed a solid pellet at the bottom of the tube, which was also difficult to resuspend after centrifugation. In addition to forming a pellet, it seemed to stick to the walls of the tube, so it was difficult to observe the volume of the pellet and to determine if some of it would have been lost in the process. Furthermore, during preparation of the standard curve using alginate dissolved in liquid LB medium, sometimes the solution foamed, and the Ca-alginate precipitated on the surface of the solution, especially at higher concentrations. This impaired discarding the supernatant without losing the alginate. These issues might offer another explanation for the high variance of the results.

For the statistical analysis of the data of three standard curves obtained from three independent experiments, a polynomial function of second degree was fitted and 95% prediction bands were calculated (Figure 9). As described in 3.2.1, the data showed high variation especially in alginate concentrations above 0.8 mg/ml. Furthermore, it was expected that the data would correspond to a linear function. However, the data corresponded better to a polynomial function of third degree than to a linear function, which might be due to high variation. The result that the data varied more at the higher concentrations than at the lower ones is surprising as Zheng et al. showed that the crystal violet assay could measure alginate in concentrations starting from 0.05 mg/ml up to around 1.5 mg/ml, showing lower accuracy for concentrations under 0.2 mg/ml (Zheng et al., 2016). Their standard curve showed a linear correlation between 0.2 and 2.0 mg/ml (Zheng et al., 2016). Figure 14 shows that this was rather the case for concentrations between 0.0 mg/ml and 0.8 mg/ml. As mentioned in previous paragraphs, aggregation of alginate by $CaCl_2$ did not work reliably, which could

be due to $CaCl_2$ interacting with another substance. Furthermore, the consistency and the occasional foaming of the aggregate led to additional variations. However, it still needs to be explained why the variation was higher at higher concentrations, i.e., above 0.8 mg/ml of alginate. Sometimes the Ca-alginate precipitated on top of the supernatant, which made it hard to discard the supernatant. This occurred more frequently when processing higher concentrations and could have caused the higher variability in these samples as well as the deviation from a linear function.

Crystal violet staining of bacterial cultures was performed according to Zheng et al., with minor modifications (Zheng et al., 2016). As for the standard curves, 1 M $CaCl_2$ was utilized, the crystal violet-stained Ca-alginate was washed with 1% acetic acid and different volumes of the crystal violet solution and centrifugation at 2000-3000 rpm were utilized in order to improve the assay (see 2.8.2). However, the reliability of the assay could not be improved with these measures. Furthermore, instead of adding $CaCl_2$ to the cultures before centrifugation, the cultures were first centrifuged, the cell pellet removed, and then $CaCl_2$ was added to the supernatant. This was implied in the experimental process in order to discard the cell pellet, but not the alginate, which otherwise could have been precipitated with the cell pellet. After the parameters of the crystal violet assay had been optimized, the results of 9 independent experiments conducted under the same conditions were compared. In all except one of those experiments, the absorbance of *P. aeruginosa* PDO300 was higher than the absorbance of the P. *aeruginosa* PAO1 sample. This is in accordance with the fact that *P. aeruginosa* PDO300 is an alginate overproducing mutant, while PAO1 does not produce alginate under aerobic conditions (Hentzer et al., 2001; Wozniak et al., 2003). However, there was great variation in the results regarding the absorbance of *P. aeruginosa* PAO1 and PDO300 and the difference in absorbance between the two strains (see Figure 12 and 3.2.3). Furthermore, the mean absorbance of *P. aeruginosa* PAO1 was at 5.3 and therefore lower than the mean absorbance of PDO300, which was at 7.6 (Figure 12). As PAO1 does not produce alginate under aerobic conditions, it was expected that its absorbance would be zero (Wozniak et al., 2003). One possible explanation for this is background signal. It is possible

that other extra- or after lysis intracellular substances other than alginate were stained by crystal violet, therefore increasing the OD_{600} such as LPS and DNA.

SadC is a diguanylate cyclase that produces the signaling molecule c-di-GMP, which is necessary for the immediate production of intermediate amounts of alginate by *P. aeruginosa* as a response to low oxygen tensions (Schmidt et al., 2016). This is a post-translational mechanism of alginate regulation (Schmidt et al., 2016). To further explore the role of *sadC* in alginate production, determining the alginate content in different *P. aeruginosa sadC* mutations could be helpful. As described at 3.2.4, two mutants of *P. aeruginosa* PAO1 with a *sadC* deletion were tested: *P. aeruginosa* PAO1Δ*sadC*, which contains an unmarked in-frame deletion of sadC, and *P. aeruginosa* PAO1*sadC*Δ*TM*, which contains a deletion of the transmembrane domain of *sadC*, but the cytoplasmic domain containing the GGDEF motif is still expressed. Zhu et al. show that a *P. aeruginosa* strain lacking the transmembrane domain of *sadC* is impaired in its ability to form a biofilm (Zhu et al., 2016). This mutant was tested in order to explore the role of the transmembrane domain and the GGDEF motif in alginate production. Both strains were grown under aerobic conditions and examined using the crystal violet assay.

The absorbance of *P. aeruginosa* PAO1 was the lowest, as in prior crystal violet staining assays, and consistent with PAO1 not producing alginate under aerobic conditions (see Figure 13) (Wozniak et al., 2003). The absorbance of *P. aeruginosa* PDO300 was the highest, which corresponded to prior experiments and to the fact that *P. aeruginosa* PDO300 is an alginate overproducing mutant (Mathee et al., 1999). Furthermore, the results show a high standard deviation. This also corresponds to prior experiments mentioned in this work that showed great variation between experiments. *P. aeruginosa* PAO1Δ*sadC* had a low absorbance similar to PAO1, while the absorbance of PAO1*sadC*Δ*TM* was approximately between the absorbance of PAO1Δ*sadC* and PDO300. According to Schmidt et al., like *P. aeruginosa* PAO1, PAO1Δ*sadC* produced minimal amounts of alginate under aerobic conditions, which is consistent with the results of this work (Schmidt et al., 2016). The intermediate absorbance of *P. aeruginosa*

PAO1*sadC*Δ*TM* is most likely due to the high variation and not an alginate overproduction caused by the deletion of the transmembrane domain.
In conclusion, the results of crystal violet staining of *sadC* mutants are consistent with previous works. However, as *sadC* promotes alginate overproduction under anaerobic conditions, the strains should be grown anaerobically in order to adequately examine *sadC* transmembrane domain activity.

To compare the crystal violet assay with other studies, the alginate concentration was calculated using linear regression (Equation 3), the coefficients depicted in Table 8 (Appendix 2), and the measured average absorbance depicted at Figure 12. The average alginate concentration was calculated. This resulted in a concentration of 198.72 μg of alginate per ml of supernatant for *P. aeruginosa* PAO1 and 312.06 μg/ml for *P. aeruginosa* PDO300. *P. aeruginosa* PAO1 is generally described as a producer of very low to no amounts of alginate under aerobic conditions (Hentzer et al., 2001; Wozniak et al., 2003). For *P. aeruginosa* PDO300, alginate concentrations of 150 μg/ml (Malhotra et al., 2000), 615,89 μg/ml (Cross & Goldberg, 2019) and 1500 μg/ml (Zheng et al., 2016) have been described. In the first two articles, a modified carbazole method was used, in the third one, the crystal violet assay. In all of the mentioned works, LB medium was used, and the growth conditions were the same, if they were mentioned in the articles (Cross & Goldberg, 2019; Malhotra et al., 2000; Zheng et al., 2016). The high variation in the alginate levels between the different studies demonstrates again that alginate measurement is challenging and that it is hard to compare its amounts between different experimental set-ups. The alginate concentration that was measured in this work lies in the scope of other published results, but it was five times lower than the concentration measured with the same technique (Zheng et al., 2016). One of the reasons why measuring *P. aeruginosa* alginate is challenging is that it is a large, complex and variable exopolysaccharide difficult to purify (Awad & Aboul-Enein, 2013; Dusseault et al., 2006). However, most established methods require an enrichment of alginate, which is why finding a method that does not require purification is so important (Østgaard, 1993; Zheng et al., 2016).

The great variation of the crystal violet assay results and the difficulties in the experimental set-up raise the question of how to improve this assay to reach adequate applicability. A first step of improving the crystal violet assay is optimizing its conditions. The supernatant needs to be pipetted very carefully to not aspirate the delicate alginate, and it needs to be resuspended thoroughly. However, as the experiment was replicated many times, these experimental steps were numerously varied and improved, which signifies that this approach does not offer great potential of optimization. Another proposition to improve the set-up is the utilization of tubes made of a different material, e.g. glass or steel. This might reduce the sticking to the side of the dyed alginate, improve observability of the pellet volume and simplify resuspension. However, this does not solve the problem of loss of alginate because it can still be poured or pipetted out. Finally, the precipitation of alginate on top of the sample could be prevented by adding an anti-foaming agent. As it is suspected that the alginate precipitates with the foam, this might inhibit foam formation and precipitation of alginate. The alginate pellet being located at the bottom of the tube facilitates the pouring out of supernatant and reduces loss of alginate. However, this might only be effective for higher concentrations as alginate did not precipitate at the surface layer in lower concentrations. Furthermore, the selection of an anti-foaming agent is often tedious and requires extensive calculations (Kato et al., 2020). In conclusion, optimization of the experimental set-up does not offer great potential to improve the variation during the experimental procedure and of the measured values.

One potential improvement is the implementation of more measuring points between 0.2 mg/ml and 0.8 mg/ml. The statistical analysis (see 2.8.3) shows that the results were more consistent in the scope of 0.2 to 0.8 mg/ml and a linear relation was given between concentration of alginate and OD. When replicating the assay another time, more measuring points (e.g. for every 0.1 mg/ml) could be implemented, which might result in a more valid calibration curve. This is especially relevant because the results of staining *P. aeruginosa* cultures were in that range, and it would improve the quality of results for lower alginate concentrations. Nevertheless, this does not solve the problem of inter-experimental variability that is depicted Figure 12. Even if a valid standard curve

is achieved, the results of measuring the alginate concentration of a *P. aeruginosa* culture might vary due to the loss of alginate.

In conclusion, the results by Zheng et al. that the crystal violet assay was reproducibly suitable for measuring concentrations of alginate starting at 0.05 mg/ml could not be reproduced, as the assay showed to much variation and the standard curve did not completely correspond to a linear relation between OD_{600} and alginate concentration (Zheng et al., 2016). Optimizing the crystal violet staining method with the aforementioned approaches might lead to a reliable standard curve and slightly enhanced replicability, but it does not solve all the obstacles that lay in the experimental procedure itself. At this time, the crystal violet assay is considered not suitable for the measurement of low alginate concentrations produced by non-mucoid isolates of *P. aeruginosa.* However, as the OD_{600} of *P. aeruginosa* PDO300 was – with one exception - always higher than the OD_{600} of PAO1 (Figure 12), the assay can potentially be used to differentiate between mucoid and non-mucoid isolates of *P. aeruginosa.*

4.3 Alcian blue staining as a qualitative approach of alginate measurement

The aim of Alcian blue staining was to find a straightforward method of detecting alginate levels at the single cell level. Wardi & Allen showed that it is possible to stain glycoproteins isolated from the brain with Alcian blue using electrophoresis (Wardi & Allen, 1972). For this work, a different approach was chosen, and bacteria were directly stained after being fixed on glass slides. As for the crystal violet assay, the experiments were conducted using wildtype *P. aeruginosa* PAO1 and PDO300. Fixation by heat as well as fixation with formaldehyde was tested. Bacteria were cultured in liquid cultures as well as on agar plates for varying incubation periods using different media.

As a first approach, *P. aeruginosa* PAO1 and PDO300 from plate cultures were suspended in water, heat fixed and stained on glass slides without being washed (see p.38), which resulted in adequate differentiability between the strains. After including a washing step before adding the dye, one experiment produced satisfactory results (see Figure 15), with blue halos surrounding several PDO300 bacteria presumably representing alginate. However, these halos were only present around some of the bacteria and not in every experiment. Frequently,

little to no difference between *P. aeruginosa* PAO1 and PDO300 was observed. However, it can be concluded that Alcian blue can stain alginate, as the only difference between *P. aeruginosa* PAO1 and PDO300 is the overproduction of alginate by PDO300 (Mathee et al., 1999). It was suspected that the heat fixation damaged the delicate hydrated matrix surrounding the bacterial cells. To avoid that, fixation with 4% formaldehyde was implemented. This approach provided differentiability: The *P. aeruginosa* PDO300 samples showed blue streaks in the background as well as blue halo-like structures like mentioned above, whereas the *P. aeruginosa* PAO1 samples had a clear, unicolour background (see Figure 15). However, these results once again could hardly be replicated.

The Alcian blue assay produced microscopically visible blue halos around individual bacteria and/or blue streaks between bacteria of the alginate overproducing mutant *P. aeruginosa* PDO300. Between aerobically grown PDO300 and the wildtype *P. aeruginosa* PAO1, a clear difference could be seen when looking at the bacteria under the microscope. However, this effect could only be observed in a small part of the experiments carried out under the same conditions. The question now arises as to whether the stained substance is actually alginate. Theoretically, it is possible that the blue streaks represent another substance present in the material scraped from the agar plates, such as the polysaccharides Pel and Psl or DNA. *P. aeruginosa* PDO300 is a mutant of *P. aeruginosa* PAO1 that expresses the *mucA22* allele, which leads to the overexpression of *algT* or *algU*, resulting in the overexpression of the alginate biosynthesis operon, which results in the production of high amounts of alginate under aerobic conditions (Mathee et al., 1999). Since this mutation is the only genetic difference between *P. aeruginosa* PAO1 and PDO300, the most obvious reason for the microscopic difference between the two strains stained with Alcian blue is that alginate was stained. To verify this, the staining can be performed with a PDO300 mutant carrying a deletion of an essential alginate synthesis gene, which should lead to a PAO1 phenotype.

As the Alcian blue assay is simple and allows observations at the single cell level, it could strongly simplify the detection of alginate production in *P. aeruginosa*, especially in non-mucoid isolates. This raises the question whether it is possible

to improve the assay so that it can be used for alginate detection in research laboratories. Reproducibility needs to be improved in order to be able to apply the Alcian blue assay in the lab. This experiment showed overall poor reproducibility, even when the conditions were kept as constant as possible. It was supposed that the heat fixation damaged the hydrate envelope which hence could not be stained. To counteract this problem, formaldehyde was used for fixation, which was proven to be functional but consistent results could still not be achieved. In conclusion, it remains unclear at the moment why the Alcian blue assay is difficult to reproduce.

4.4 Comparison of different methods of alginate measurement

In the last paragraphs, the benefits and disadvantages of the methods that were investigated in this work were discussed. In the following paragraphs the crystal violet assay, the Alcian blue assay, and the carbazole assay will be compared from different aspects.

Firstly, the three assays differ in terms of sensitivity. The carbazole assay is an established assay that is very sensitive compared to the crystal violet assay (Zheng et al., 2016), but the crystal violet assay is still sensitive enough to detect alginate concentrations starting at 0.2 mg/ml (see Figure 10). The sensitivity of the Alcian blue assay is more difficult to examine, as *P. aeruginosa* PDO300 and *P. aeruginosa* PAO1 were the only strains that were analysed. To determine the lowest concentration of alginate that can be measured with the Alcian blue assay, it would be necessary to analyse other strains or alginate solutions, which would be a tedious task due to the low reliability of the Alcian blue assay. Therefore, it is likely that the carbazole assay is the most sensitive amongst the three assays.

Secondly, the ease of use needs to be considered. All the assays can be conducted in most labs and do not require special equipment. The crystal violet assay is a bit more difficult to perform as the supernatant needs to be pipetted very carefully (see 4.2), compared to the Alcian blue assay which is very fast and easy to do. These assays do not require hazardous chemicals, whereas the carbazole assay involves carbazole and concentrated sulfuric acid (Bitter & Muir, 1962; Dische, 1947). Furthermore, the alginate needs to be enriched or purified first in order to be measured by the carbazole assay to avoid background noise

(Frazier et al., 2008; Zheng et al., 2016). These factors contribute to the desire to develop an assay that could replace the carbazole assay as the standard method of alginate detection. The Alcian blue assay is the most user-friendly amongst the three. Thirdly, an aim of this work was to find a method that was suitable for comparing the alginate production at the single cell level. This is possible with Alcian blue staining, a microscopic method, but not with the other two methods. Finally, the assays differ in terms of reliability. The carbazole assay is susceptible to background noise (Frazier et al., 2008; Zheng et al., 2016), but shows high specificity towards uronic acids (Knutson & Jeanes, 1968). Moreover, as the carbazole assay has been used for over 70 years, a lot of experience with this method exists (Dische, 1947). Still, as mentioned in 4.1, other authors' work shows some variation in results. As mentioned under 3.2, the crystal violet assay produced overall inconsistent results, displaying high inter-experimental variability and poor reliability. The Alcian blue assay showed similar difficulties, with multiple experiments failing to enable distinguishing between the different *P. aeruginosa* strains, as well as insufficient reliability.

In conclusion, neither the crystal violet nor the Alcian blue assay are currently appropriate for measuring and detecting higher and intermediate alginate concentrations, respectively. Nevertheless, the carbazole method has its own difficulties and disadvantages and it remains crucial to find an easy, practical and reliable method of alginate detection.

4.5 Fourier transform infrared spectroscopy as a potential new method of alginate measurement

One promising method of alginate measurement is Fourier transform infrared spectroscopy (FT-IR), which was explored by Correa et al. and demonstrated to be a practical, valid, and efficient method to quantify alginate (Correa et al., 2012). Different mutants of *Pseudomonas fluorescens* were tested, while an alginate-producing mutant *P. fluorescens* SBW25 was used as a reference strain (Correa et al., 2012). FT-IR was performed as follows: Bacterial cultures were pipetted onto a 96-well-plate and infrared absorbance spectra were measured in different locations of the sample in a spectrometer (Correa et al., 2012). Signal-to-noise ratio was improved by adding interferograms and the data were converted to

ASCII format (Correa et al., 2012). Subsequently, the data were filtered in order to omit low quality and unreproducible spectra, outliers were eliminated, and the remaining spectra were normalized by an extended multiplicative signal correction (EMSC) algorithm (Correa et al., 2012). The multivariate data analysis technique of canonical variates analysis was used to determine the relationship between bacterial growth, alginate production and FT-IR spectra (Correa et al., 2012). To examine the ability of the experiment to quantify alginate, a mathematic model, specifically a multi-variate partial least squares regression (PLSR), that calculated alginate concentrations using the FT-IR spectra was established (Correa et al., 2012). The alginate concentration was between 2.65 and 9.00 g/l (Correa et al., 2012). These values were compared with the results of an enzymatic alginate assay that acted as a control group (Correa et al., 2012; Østgaard, 1993). This assay utilizes alginate lyases that cleave alginate, leaving a uronic acid end, which absorbs light at 230-240 nm and can be measured photometrically (Østgaard, 1993). The normalized root-mean-square error of the method was approximately 14.5%, depending on the growth medium (Correa et al., 2012). The validity of the method was tested further using various validation methods (Correa et al., 2012). The benefits of alginate quantification by FT-IR can be summarized as following: First, no reagents are needed, most importantly no hazardous chemicals (Correa et al., 2012). Second, purification is not necessary, and the sample stays intact and can be used in other experiments (Correa et al., 2012). Furthermore, a biochemical fingerprint of the sample is generated which offers further information without other tests needing to be performed, thus providing a high yield of information in one single test (Correa et al., 2012). Last, the method shows great accuracy (Correa et al., 2012). However, there are also disadvantages to this method that need to be mentioned: An infrared spectrometer is necessary, which is neither already available in most labs, nor inexpensive. In order to quantify alginate, the FT-IR data requires extensive analysis and programming skills (Correa et al., 2012). Therefore, a prolonged period of preparatory work and training might be necessary to successfully implement FT-IR in habitual use. Furthermore, the FT-IR assay would have to be replicated with *P. aeruginosa.* While a concentration of alginate

produced by *P. fluorescens* between 2.65 and 9.00 g/l was measured with FT-IR quantification, the concentration of alginate produced by *P. aeruginosa* PDO300 was measured at 0.15 to 0.62 g/l in other studies (Correa et al., 2012; Cross & Goldberg, 2019; Malhotra et al., 2000). The concentration of alginate produced by non-mucoid *P. aeruginosa* would be even lower, therefore it needs to be tested if FT-IR is sensitive enough for such alginate levels.

In conclusion, all methods that were compared and discussed in this work show their own advantages and disadvantages. Depending on the laboratory setting in which alginate testing is performed, a suitable method needs to be selected. Further research and testing of alginate detection methods is of great importance for *P. aeruginosa* and CF research.

5 Summary

Cystic fibrosis is a life-limiting genetic condition that affects multiple organ systems, lung disease usually being the main contributor to disease and mortality. The cause for CF is a defective ion channel called CFTR, which leads to altered ion concentration, dehydrated, sticky mucus in the airways, impaired mucociliary clearance and weakened pulmonary immune defense. This promotes early and chronic airway infection, *Pseudomonas aeruginosa* being the predominant pathogen in adult CF patients and contributing strongly to lung disease severity. It is highly capable of adapting to the CF lung environment. Due to mutations the bacteria can for example convert to a mucoid phenotype that is caused by the overproduction of the exopolysaccharide alginate. That mucoid conversion allows for the formation of a biofilm which contributes to the difficulty to permanently eradicate *P. aeruginosa* during the chronic stage of infection. As alginate production is the hallmark of chronic *P. aeruginosa* infection of CF patients, further research of the polysaccharide is of great importance and a sensitive, user-friendly method of alginate measurement is crucial for CF research. However, *P. aeruginosa* alginate is a complex polysaccharide that is acetylated, of variable composition and difficult to purify to high purity. Furthermore, anoxic conditions - which are found in the CF lung - have been shown to stimulate alginate production in non-mucoid *P. aeruginosa*. Several methods to measure and detect alginate exist, however, they all have different advantages and disadvantages, such as the requirement of expensive equipment or hazardous chemicals. The aim of this work was to find a sensitive and user-friendly method for the measurement of alginate produced by *P. aeruginosa* by testing a recently published crystal violet staining technique and the Alcian blue dye for staining alginate on *P. aeruginosa* cells. First, it was analyzed if the anoxia-induced increase in alginate production by the non-mucoid PAO1 strain can be macroscopically detected similar to mucoid isolates with a slimy colony appearance. Indeed, after incubation on modified M9 agar plates under anaerobic conditions, PAO1 colonies showed a more mucoid appearance than the aerobically grown bacteria. This assay could be used as crude technique to differentiate between alginate non-producers and producers. However, it does

not allow for a quantification of alginate. Second, the spectrophotometric crystal violet assay was tested for suitability and reproducibility using *P. aeruginosa* strains producing different levels of alginate. A standard curve of crystal violet-stained purified commercially available alginate at concentrations ranging from 0.0 to 2.0 mg/ml was prepared. Statistical analysis showed that there was a linear relation between the concentrations up to 0.8 mg/ml but high variation at higher concentrations. Using *P. aeruginosa* cultures to measure alginate concentrations with this technique showed that there was a considerable variability between experiments and a lack of reproducibility, which could be due to the experimental procedure. Thus, this technique was considered not suitable for reliable measurements of alginate concentrations.

Finally, it was tested whether the Alcian blue dye could be used to stain and microscopically detect alginate on *P. aeruginosa* bacteria. Blue halo-like structures around some of the *P. aeruginosa* PDO300 bacteria were microscopically observed. These were absent from PAO1 bacteria suggesting that the structures represent the alginate matrix surrounding the bacteria. With this assay, it was also possible to observe alginate production at the single cell level albeit some variation between and within experiments. The major disadvantage of both the crystal violet and the Alcian blue assay is the inconsistent and highly variable results. Even though both are fast, straightforward and do not require special equipment or hazardous chemicals, they are currently not as reliable as other established methods. Some potential lies in further optimization of both assays but is to be doubted that this will lead to a great improvement in reliability. A novel, sensitive method of alginate measurement is Fourier transform infrared spectroscopy, which should be further explored in the future.

6 Deutsche Zusammenfassung

Mukoviszidose (auch: Zystische Fibrose) ist eine lebensbedrohliche genetische Krankheit, die multiple Organsysteme betrifft, wobei die Lungenbeteiligung zumeist der entscheidende Faktor für die Krankheitsschwere und Mortalität ist. Die Ursache der Mukoviszidose ist der defekte Ionenkanal CFTR, der eine Veränderung der Ionenkonzentration, dehydrierten, klebrigen Schleim in den Atemwegen, eine Störung der mukoziliären Clearance und eine Schwächung der pulmonalen Immunabwehr verursacht. Dies begünstigt frühe und chronische Atemwegsinfektionen, wobei *Pseudomonas aeruginosa* das vorherrschende Pathogen bei erwachsenen Mukoviszidose-Patient:innen ist und maßgeblich zur Krankheitsschwere beiträgt. Es kann sich sehr gut an die veränderte Umgebung der von Mukoviszidose betroffenen Lunge anpassen. Durch Mutationen können die Bakterien beispielsweise zu einem mukoiden Phänotyp konvertieren, der durch die Überproduktion des Exopolysaccharids Alginat verursacht ist. Diese mukoide Konversion ermöglicht die Bildung eines Biofilms, der zur Schwierigkeit beiträgt, *P. aeruginosa* im chronischen Stadium der Infektion zu eradizieren. Da die Alginatproduktion das Kennzeichen der chronischen *P. aeruginosa*-Infektion bei Mukoviszidose-Patient:innen darstellt, ist für die Mukoviszidose-Forschung eine weitere Erforschung des Polysaccharids von hoher Wichtigkeit und eine sensitive, einfach anzuwendende Messmethode ist unabdingbar. Allerdings ist von *P. aeruginosa* produziertes Alginat ein komplexes, acetyliertes Polysaccharid, das zudem eine variable Komposition aufweist und schwer zu einem hohen Reinheitsgrad aufzureinigen ist. Des Weiteren wurde gezeigt, das anoxische Bedingungen, die in der Lunge von Mukoviszidose-Patient:innen zu finden sind, die Alginatproduktion nicht-mukoider Stämme von *P. aeruginosa* stimulieren. Es existieren bereits einige Methoden zur Messung und Detektion von Alginat, die allerdings alle verschiedene Vor- und Nachteile aufweisen. Das Ziel dieser Arbeit war es, durch die Testung einer kürzlich publizierten Kristallviolettfärbung und von Alcianblau zur Anfärbung von Alginat auf *P. aeruginosa*-Zellen, eine sensitive und anwenderfreundliche Methode für die Messung durch *P. aeruginosa* produzierten Alginats zu finden.

Zunächst wurde analysiert ob die Anoxie-induzierte Zunahme der Alginatproduktion durch den nicht-mukoiden PAO1-Stamm makroskopisch detektiert werden konnte, ähnlich wie bei mukoiden Isolaten, deren Kolonien schleimig aussehen. In der Tat zeigten PAO1-Kolonien nach Inkubierung auf modifizierten M9-Agarplatten unter anaeroben Bedingungen ein mukoideres Aussehen als aerob angezüchtete Bakterien. Dieser Versuch könnte als simple Methode zur Differenzierung von Alginatproduzenten und nicht-Produzenten dienen. Er bietet jedoch nicht die Möglichkeit der Alginatquantifizierung.

Danach wurde die spektrophotometrische Kristallviolett-Methode auf ihre Eignung und Reproduzierbarkeit getestet, wofür *P. aeruginosa*-Stämme verwendet wurden, die verschiedene Mengen an Alginat produzierten. Eine Standardkurve von Kristallviolett-gefärbtem aufgereinigtem kommerziell verfügbarem Alginat in Konzentrationen zwischen 0,0 und 2,0 mg/ml wurde vorbereitet. Die statistische Analyse zeigte ein lineares Verhältnis zwischen den Konzentrationen und der Absorption bis 0,8 mg/ml, aber auch hohe Schwankungen in den höheren Konzentrationen. Die Verwendung von *P. aeruginosa*-Kulturen zur Messung von Alginatkonzentrationen mit dieser Technik zeigte eine beachtliche inter-experimentelle Variabilität und mangelnde Reproduzierbarkeit, was an dem experimentellen Verfahren liegen könnte. Dementsprechend wurde diese Technik nicht als geeignet für verlässliche Messungen von Alginatkonzentrationen angesehen.

Zuletzt wurde untersucht, ob Alcianblau-Farbe zur Anfärbung und mikroskopischen Detektion von Alginat auf *P. aeruginosa*-Bakterien verwendet werden kann. Blaue lichthofartige Strukturen, die manche der *P. aeruginosa* PDO300-Bakterien umgaben, wurden unter dem Mikroskop betrachtet. Diese zeigten sich nicht bei den PAO1-Bakterien, was darauf schließen lässt, dass diese Strukturen die Alginatmatrix repräsentieren, die die Bakterien umgibt. Mit dieser Methode war es auch möglich, die Alginatproduktion auf Einzellzellebene zu beobachten, wenn auch eine gewisse Schwankung zwischen den Experimenten und innerhalb der Experimente auftrat. Der größte Nachteil der Kristallviolett- und der Alcianblau-Technik sind die inkonsistenten und schwankenden Ergebnisse. Auch wenn beide Techniken schnell und

unkompliziert sind und weder spezielle Ausstattung noch gefährliche Chemikalien benötigen, sind sie momentan nicht so verlässlich wie andere etablierte Methoden. Es liegt zwar Potential in der weiteren Optimierung beider Techniken, allerdings ist anzuzweifeln, dass dies zu einer starken Verbesserung der Zuverlässigkeit führt. Eine neuartige, sensitive Methode zur Alginatmessung ist Fourier-transformierte Infrarotspektroskopie, die in Zukunft weiter erforscht werden sollte.

7 References

Ahmar, R. Al, Kirby, B. D., & Yu, H. D. (2020). Culture of Small Colony Variant of Pseudomonas aeruginosa and Quantitation of its Alginate. *J Vis Exp*, *156*(February), 1–8. https://doi.org/10.3791/60466

Aitken, E., Cheema, A., Elliott, S., & Khan, S. (2011). Different Compositions of Biofilm Extracellular Polymeric Substance Reveals Contrasting Antibiotic Resistance Profiles in Pseudomonas aeruginosa. *Microbiology and Immunology*, *15*(April), 79–83.

Alton, E. W., Armstrong, D. K., Ashby, D., Bayfield, K. J., Bilton, D., Bloomfield, E. V, Boyd, A. C., Brand, J., Buchan, R., Calcedo, R., Carvelli, P., Chan, M., Cheng, S. H., Collie, D. S., Cunningham, S., Davidson, H. E., Davies, G., Davies, J. C., Davies, L. A., … Wolstenholme-Hogg, P. (2016). A randomised, double-blind, placebo-controlled trial of repeated nebulisation of non-viral cystic fibrosis transmembrane conductance regulator (CFTR) gene therapy in patients with cystic fibrosis. *Efficacy and Mechanism Evaluation*, *3*(5), 1–210. https://doi.org/10.3310/eme03050

Ashby, RD. (1994). The Production and Characterization of Alginate Produced by Pseudomonas Syringae. *LSU Historical Dissertations and Theses*, *5775*. https://repository.lsu.edu/gradschool_disstheses/5775

Awad, H., & Aboul-Enein, H. Y. (2013). A validated HPLC assay method for the determination of sodium alginate in pharmaceutical formulations. *Journal of Chromatographic Science*, *51*(3), 208–214. https://doi.org/10.1093/chromsci/bms129

Bhagirath, A. Y., Li, Y., Somayajula, D., Dadashi, M., Badr, S., & Duan, K. (2016). Cystic fibrosis lung environment and Pseudomonas aeruginosa infection. *BMC Pulmonary Medicine*, *16*(1), 1–22. https://doi.org/10.1186/s12890-016-0339-5

Bitter, T., & Muir, H. M. (1962). A modified uronic acid carbazole reaction. *Analytical Biochemistry*, *4*(4), 330–334. https://doi.org/10.1016/0003-2697(62)90095-7

Boyd, A., & Chakrabarty, A. M. (1995). Pseudomonas aeruginosa biofilms: role of the alginate exopolysaccharide. *Journal of Industrial Microbiology*, *15*(3), 162–168. https://doi.org/10.1007/BF01569821

Bragonzi, A., Worlitzsch, D., Pier, G. B., Timpert, P., Ulrich, M., Hentzer, M., Andersen, J. B., Givskov, M., Conese, M., & Döring, G. (2005). Nonmucoid Pseudomonas aeruginosa Expresses Alginate in the Lungs of Patients with Cystic Fibrosis and in a Mouse Model. *The Journal of Infectious Diseases*, *192*(3), 410–419. https://academic.oup.com/jid/article/192/3/410/833994

Chitnis, C. E., & Ohman, D. E. (1993). Genetic analysis of the alginate biosynthetic gene cluster of Pseudomonas aeruginosa shows evidence of an operonic structure. *Molecular Microbiology*, *8*(3), 583–590. https://doi.org/10.1111/j.1365-2958.1993.tb01602.x

Correa, E., Sletta, H., Ellis, D. I., Hoel, S., Ertesvåg, H., Ellingsen, T. E., Valla, S., & Goodacre, R. (2012). Rapid reagentless quantification of alginate biosynthesis in Pseudomonas fluorescens bacteria mutants using FT-IR spectroscopy coupled to multivariate partial least squares regression. *Analytical and Bioanalytical Chemistry*, *403*(9), 2591–2599. https://doi.org/10.1007/s00216-012-6068-6

Costerton, J. W., Stewart, P. S., & Greenberg, E. P. (1999). Bacterial biofilms: A common cause of persistent infections. *Science*, *284*(5418), 1318–1322. https://doi.org/10.1126/science.284.5418.1318

Cramer, N., Klockgether, J., & Tümmler, B. (2023). Microevolution of Pseudomonas aeruginosa in the airways of people with cystic fibrosis. *Current Opinion in Immunology*, *83*. https://doi.org/10.1016/j.coi.2023.102328

Cross, A. R., & Goldberg, J. B. (2019). Remodeling of o antigen in mucoid pseudomonas aeruginosa via transcriptional repression of wzz2. *MBio*, *10*(1). https://doi.org/10.1128/mBio.02914-18

Cystic Fibrosis Foundation. (2019). *2019 Cystic Fibrosis Foundation Patient Registry Highlights*. https://www.cff.org/sites/default/files/2021-10/2019-Cystic-Fibrosis-Foundation-Patient-Registry-Highlights.pdf

Davies, J. C., Alton, E. W. F. W., & Bush, A. (2007). Cystic fibrosis. *British Medical Journal*, *335*, 1255–1259. https://doi.org/10.1136/bmj.39391.713229.AD

Davis, P. B. (2006). Cystic fibrosis since 1938. *American Journal of Respiratory and Critical Care Medicine*, *173*(5), 475–482. https://doi.org/10.1164/rccm.200505-840OE

Dische, Z. (1947). A new specific color reaction of hexuronic acids. *The Journal of Biological Chemistry*, *167*(1), 189–198. http://www.ncbi.nlm.nih.gov/pubmed/20281638

Dusseault, J., Tam, S. K., Ménard, M., Polizu, S., Jourdan, G., Yahia, L., & Hallé, J. P. (2006). Evaluation of alginate purification methods: Effect on polyphenol, endotoxin, and protein contamination. *Journal of Biomedical Materials Research - Part A*, *76*(2), 243–251. https://doi.org/10.1002/jbm.a.30541

Elborn, J. S. (2016). Cystic fibrosis. *The Lancet*, *388*(10059), 2519–2531. https://doi.org/10.1016/S0140-6736(16)00576-6

Franklin, M. J., Nivens, D. E., Weadge, J. T., & Lynne Howell, P. (2011). Biosynthesis of the pseudomonas aeruginosa extracellular polysaccharides, alginate, Pel, and Psl. *Frontiers in Microbiology*, *2*(AUG), 1–16. https://doi.org/10.3389/fmicb.2011.00167

Frazier, S. B., Roodhouse, K. A., Hourcade, D. E., & Zhang, L. (2008). The Quantification of Glycosaminoglycans: A Comparison of HPLC, Carbazole,

and Alcian Blue Methods. *Open Glycoscience*, *1*, 31–39. https://doi.org/10.2174/1875398100801010031

Frederiksen, B., Koch, C., & Høiby, N. (1997). Antibiotic treatment of initial colonization with Pseudomonas aeruginosa postpones chronic infection and prevents deterioration of pulmonary function in cystic fibrosis. *Pediatric Pulmonology*, *23*(5), 330–335. https://doi.org/10.1002/(SICI)1099-0496(199705)23:5<330::AID-PPUL4>3.0.CO;2-O

Gacesa, P. (1988). Alginates. *Carbohydrate Polymers*, *8*(3), 161–182. https://doi.org/10.1016/0144-8617(88)90001-X

Garner, C. V., DesJardins, D., & Pier, G. B. (1990). Immunogenic properties of Pseudomonas aeruginosa mucoid exopolysaccharide. *Infection and Immunity*, *58*(6), 1835–1842. https://doi.org/10.1128/iai.58.6.1835-1842.1990

Govan, J. R., & Deretic, V. (1996). Microbial pathogenesis in cystic fibrosis: mucoid Pseudomonas aeruginosa and Burkholderia cepacia. *Microbiological Reviews*, *60*(3), 539–574. https://doi.org/10.1128/mr.60.3.539-574.1996

Griese, M., Costa, S., Linnemann, R. W., Mall, M. A., McKone, E. F., Polineni, D., Quon, B. S., Ringshausen, F. C., Taylor-Cousar, J. L., Withers, N. J., Moskowitz, S. M., & Daines, C. L. (2021). Safety and efficacy of elexacaftor/tezacaftor/ivacaftor for 24 weeks or longer in people with cystic fibrosis and one or more F508del alleles: Interim results of an open-label phase 3 clinical trial. *American Journal of Respiratory and Critical Care Medicine*, *203*(3), 381–385. https://doi.org/10.1164/RCCM.202008-3176LE/SUPPL_FILE/DISCLOSURES.PDF

Hanna, S. L., Sherman, N. E., Kinter, M. T., & Goldberg, J. B. (2000). Comparison of proteins expressed by Pseudomonas aeruginosa strains representing initial and chronic isolates from a cystic fibrosis patient : an analysis by 2-D gel electrophoresis and capillary column liquid chromatography-tandem mass spectrometry. *Microbiology*, *146*, 2495–2508. www.pseudomonas.com

Hassett, D. J., Sutton, M. D., Schurr, M. J., Herr, A. B., Caldwell, C. C., & Matu, J. O. (2009). Pseudomonas aeruginosa hypoxic or anaerobic biofilm infections within cystic fibrosis airways. *Trends in Microbiology*, *17*(3), 130–138. https://doi.org/10.1016/j.tim.2008.12.003

Häussler, S. (2010). Multicellular signalling and growth of Pseudomonas aeruginosa. In *International Journal of Medical Microbiology* (Vol. 300, Issue 8, pp. 544–548). https://doi.org/10.1016/j.ijmm.2010.08.006

Hay, I. D., Wang, Y., Moradali, M. F., Rehman, Z. U., & Rehm, B. H. A. (2014). Genetics and regulation of bacterial alginate production. *Environmental Microbiology*, *16*(10), 2997–3011. https://doi.org/10.1111/1462-2920.12389

Hentzer, M., Teitzel, G. M., Balzer, G. J., Heydorn, A., Molin, S., Givskov, M., & Parsek, M. R. (2001). Alginate overproduction affects pseudomonas aeruginosa biofilm structure and function. *Journal of Bacteriology*, *183*(18), 5395–5401. https://doi.org/10.1128/JB.183.18.5395-5401.2001

Herzog, C., Ballmann, M., Bargon, J., Bollmann, A., Dittrich-Weber, H., Dockter, G., Griese, M., Hüls, G., Lindemann, H., Schüler, D., & Tümmler, B. (2004). *Mukoviszidose - Zystische Fibrose* (H. Lindemann, B. Tümmler, & G. Dockter, Eds.; 4th ed.). Georg Thieme Verlag KG.

Hogardt, M., & Heesemann, J. (2010). Adaptation of Pseudomonas aeruginosa during persistence in the cystic fibrosis lung. *International Journal of Medical Microbiology*, *300*(8), 557–562. https://doi.org/10.1016/j.ijmm.2010.08.008

Holloway, B. W. (1955). Genetic Recombination in Pseudomonas aeruginosa. *J. Gen. Microbiol*, *13*, 572–581.

Jacobs, H. M., O'Neal, L., Lopatto, E., Wozniak, D. J., Bjarnsholt, T., & Parsek, M. R. (2022). Mucoid Pseudomonas aeruginosa Can Produce Calcium-Gelled Biofilms Independent of the Matrix Components Psl and CdrA. *Journal of Bacteriology*, *204*(5). https://doi.org/10.1128/jb.00568-21

Joris, L., Dab, lSI, & Quinton, P. M. (1993). Elemental Composition of Human Airway Surface Fluid in Healthy and Diseased Airways. *Am Rev Respir Dis*, *148*, 1633–1637.

Kato, Y., Osawa, T., Yoshihara, M., Fujii, H., Tsutsumi, S., & Yamamoto, H. (2020). Evaluation of the Antifoaming Effect Using Hansen Solubility Parameters. *ACS Omega*, *5*(11), 5684–5690. https://doi.org/10.1021/acsomega.9b03567

Kerem, B., Rommens, J. M., Buchanan, J. A., Markiewicz, D., Cox, T. K., Chakravarti, A., Buchwald, M., & Tsui, L. C. (1989). Identification of the cystic fibrosis gene: genetic analysis. *Science*, *245*(4922), 1073–1080. https://doi.org/10.1126/science.2570460

Kipnis, E., Sawa, T., & Wiener-Kronish, J. (2006). Targeting mechanisms of Pseudomonas aeruginosa pathogenesis. *Medecine et Maladies Infectieuses*, *36*(2), 78–91. https://doi.org/10.1016/j.medmal.2005.10.007

Knutson, C. A., & Jeanes, A. (1968). A new modification of the carbazole analysis: Application to heteropolysaccharides. *Analytical Biochemistry*, *24*(3), 470–481. https://doi.org/10.1016/0003-2697(68)90154-1

Kunzelmann, K. (2003). ENaC is inhibited by an increase in the intracellular Cl- concentration mediated through activation of Cl-channels. *Pflugers Arch-Eur J Physiol*, *445*, 504–512. https://doi.org/10.1007/s00424-002-0958-y

Liu, J., Yang, S., Li, X., Yan, Q., Reaney, M. J. T., & Jiang, Z. (2019). Alginate Oligosaccharides: Production, Biological Activities, and Potential Applications. *Comprehensive Reviews in Food Science and Food Safety*, *18*(6), 1859–1881. https://doi.org/10.1111/1541-4337.12494

Long, F. R., Williams, R. S., & Castile, R. G. (2004). Structural airway abnormalities in infants and young children with cystic fibrosis. *Journal of Pediatrics*, *144*(2), 154–161. https://doi.org/10.1016/j.jpeds.2003.09.026

Malhotra, S., Silo-Suh, L. A., Mathee, K., & Ohman, D. E. (2000). Proteome Analysis of the Effect of Mucoid Conversion on Global Protein Expression in Pseudomonas aeruginosa Strain PAO1 Shows Induction of the Disulfide Bond Isomerase, DsbA. *Journal of Bacteriology*, *182*(24), 6999–7006.

Marcus, H., & Baker, N. R. (1985). Quantitation of adherence of mucoid and nonmucoid Pseudomonas aeruginosa to hamster tracheal epithelium. *Infection and Immunity*, *47*(3), 723–729. https://doi.org/10.1128/iai.47.3.723-729.1985

Marson, F. A. L., Bertuzzo, C. S., & Ribeiro, J. D. (2016). Classification of CFTR mutation classes. *The Lancet. Respiratory Medicine*, *4*(8), e37–e38. https://doi.org/10.1016/S2213-2600(16)30188-6

Mathee, K., Ciofu, O., Sternberg, C., Lindum, P. W., Campbell, J. I. A., Jensen, P., Johnsen, A. H., Givskov, M., Ohman, D. E., Molin, S., Høiby, N., & Kharazmi, A. (1999). Mucoid conversion of Pseudomonas aeruginosa by hydrogen peroxide: A mechanism for virulence activation in the cystic fibrosis lung. *Microbiology*, *145*(6), 1349–1357. https://doi.org/10.1099/13500872-145-6-1349

Matsui, H., Grubb, B. R., Tarran, R., Randell, S. H., Gatzy, J. T., Davis, C. W., & Boucher, R. C. (1998). Evidence for periciliary liquid layer depletion, not abnormal ion composition, in the pathogenesis of cystic fibrosis airways disease. *Cell*, *95*(7), 1005–1015. https://doi.org/10.1016/S0092-8674(00)81724-9

Mehta, A. (2005). CFTR: More than just a chloride channel. *Pediatric Pulmonology*, *39*(4), 292–298. https://doi.org/10.1002/ppul.20147

Mulani, M. S., Kamble, E. E., Kumkar, S. N., Tawre, M. S., & Pardesi, K. R. (2019). Emerging strategies to combat ESKAPE pathogens in the era of antimicrobial resistance: A review. *Frontiers in Microbiology*, *10*(APR). https://doi.org/10.3389/FMICB.2019.00539/FULL

Munck, A., Phane Bonacorsi, S. Â., Mariani-Kurkdjian, P., Lebourgeois, M., Le Ge, M. Á., Rardin, Â., Brahimi, N. È., Navarro, J., & Bingen, E. (2001). Genotypic Characterization of Pseudomonas aeruginosa Strains Recovered From Patients With Cystic Fibrosis After Initial and Subsequent Colonization. *Pediatric Pulmonology*, *32*, 288–292.

Nikaido, H. (1994). Prevention of Drug Access to Bacterial Targets: Permeability Barriers and Active Efflux , Hiroshi Nikaido. *Science*, *264*(5157), 382–388. https://www.science.org

Nivens, D. E., Ohman, D. E., Williams, J., & Franklin, M. J. (2001). Role of alginate and its O acetylation in formation of Pseudomonas aeruginosa

microcolonies and biofilms. *Journal of Bacteriology*, *183*(3), 1047–1057. https://doi.org/10.1128/JB.183.3.1047-1057.2001

Østgaard, K. (1993). Determination of alginate composition by a simple enzymatic assay. *Hydrobiologia*, *260–261*(1), 513–520. https://doi.org/10.1007/BF00049064

O'Sullivan, B. P., & Freedman, S. D. (2009). Cystic fibrosis. *The Lancet*, *373*(9678), 1891–1904. https://doi.org/10.1016/S0140-6736(09)60327-5

Page, W. J., & Sadoff, H. L. (1975). Relationship between calcium and uronic acids in the encystment of Azotobacter vinelandii. *Journal of Bacteriology*, *122*(1), 145–151. https://doi.org/10.1128/jb.122.1.145-151.1975

Pape, H.-C., Kurtz, A., Silbernagl, S., Klinke, R., Bleich, M., Draguhn, A., Ehmke, H., & Singer, D. (2023). *Physiologie* (H.-C. Pape, A. Kurtz, & S. Silbernagl, Eds.; 10th ed., Vol. 10). Thieme, Stuttgart.

Pier, G. B., Coleman, F., Grout, M., Franklin, M., & Ohman, D. E. (2001). Role of alginate O acetylation in resistance of mucoid Pseudomonas aeruginosa to opsonic phagocytosis. *Infection and Immunity*, *69*(3), 1895–1901. https://doi.org/10.1128/IAI.69.3.1895-1901.2001

Pritchard, M. F., Powell, L. C., Adams, J. Y. M., Menzies, G., Khan, S., Tøndervik, A., Sletta, H., Aarstad, O., Skjåk-Bræk, G., McKenna, S., Buurma, N. J., Farnell, D. J. J., Rye, P. D., Hill, K. E., & Thomas, D. W. (2023). Structure–Activity Relationships of Low Molecular Weight Alginate Oligosaccharide Therapy against Pseudomonas aeruginosa. *Biomolecules*, *13*(9). https://doi.org/10.3390/biom13091366

Qin, S., Xiao, W., Zhou, C., Pu, Q., Deng, X., Lan, L., Liang, H., Song, X., & Wu, M. (2022). Pseudomonas aeruginosa: pathogenesis, virulence factors, antibiotic resistance, interaction with host, technology advances and emerging therapeutics. *Signal Transduction and Targeted Therapy*, *7*(1). https://doi.org/10.1038/s41392-022-01056-1

Riordan, J. R., Rommens, J. M., Kerem, B., Alon, N., Rozmahel, R., Grzelczak, Z., Zielenski, J., Lok, S., Plavsic, N., Chou, J. L., & Al., E. (1989). Identification of the cystic fibrosis gene: cloning and characterization of complementary DNA. *Science*, *245*(4922), 1066–1073. https://doi.org/10.1126/science.2475911

Schleheck, D., Barraud, N., Klebensberger, J., Webb, J. S., & Mcdougald, D. (2009). Pseudomonas aeruginosa PAO1 Preferentially Grows as Aggregates in Liquid Batch Cultures and Disperses upon Starvation. *PLoS ONE*, *4*(5), 5513. https://doi.org/10.1371/journal.pone.0005513

Schmidt, A., Hammerbacher, A. S., Bastian, M., Nieken, K. J., Klockgether, J., Merighi, M., Lapouge, K., Poschgan, C., Kölle, J., Acharya, K. R., Ulrich, M., Tümmler, B., Unden, G., Kaever, V., Lory, S., Haas, D., Schwarz, S., & Döring, G. (2016). Oxygen-dependent regulation of c-di-GMP synthesis by SadC controls alginate production in Pseudomonas aeruginosa.

Environmental Microbiology, *18*(10), 3390–3402. https://doi.org/10.1111/1462-2920.13208

Singh, P. K., Schaefer, A. L., Parsek, M. R., Moninger, T. O., Welsh, M. J., & Greenberg, E. P. (2000). Quorum-sensing signals indicate that cystic fibrosis lungs are infected with bacterial biofilms. *Nature*, *407*(6805), 762–764. https://doi.org/10.1038/35037627

Smith, J. J., Travis, S. M., Greenberg, E. P., & Welsh, M. J. (1996). Cystic fibrosis airway epithelia fail to kill bacteria because of abnormal airway surface fluid. *Cell*, *85*(2), 229–236. https://doi.org/10.1016/S0092-8674(00)81099-5

Sommerburg, O., & Mall, M. A. (2022). Mukoviszidose. In M. Kreuter, U. Costabel, F. J. Herth, & D. Kirsten (Eds.), *Seltene Lungenerkrankungen* (2nd ed., Vol. 2, pp. 389–401). Springer-Verlag Berlin. https://doi.org/10.1007/978-3-662-63651-0

Theilacker, C., Coleman, F. T., Mueschenborn, S., Llosa, N., Grout, M., & Pier, G. B. (2003). Construction and characterization of a Pseudomonas aeruginosa mucoid exopolysaccharide-alginate conjugate vaccine. *Infection and Immunity*, *71*(7), 3875–3884. https://doi.org/10.1128/IAI.71.7.3875-3884.2003

Vogelberg, C., & Seidenberg, J. (2022). *Pädiatrische Pneumologie* (C. Vogelberg & J. Seidenberg, Eds.). De Gruyter. https://doi.org/doi:10.1515/9783110693454

Wang, Y. (2017). *Understanding aspects of alginate biosynthesis and regulation by Pseudomonas aeruginosa* [PhD]. Massey University.

Wardi, A. H., & Allen, W. S. (1972). Alcian blue staining of glycoproteins. *Analytical Biochemistry*, *48*(2), 621–623. https://doi.org/10.1016/0003-2697(72)90118-2

Wilhelm, M. J., Sharifian Gh., M., Wu, T., Li, Y., Chang, C. M., Ma, J., & Dai, H. L. (2021). Determination of bacterial surface charge density via saturation of adsorbed ions. *Biophysical Journal*, *120*(12), 2461–2470. https://doi.org/10.1016/j.bpj.2021.04.018

Winstanley, C., O'Brien, S., & Brockhurst, M. A. (2016). Pseudomonas aeruginosa Evolutionary Adaptation and Diversification in Cystic Fibrosis Chronic Lung Infections. *Trends in Microbiology*, *24*(5), 327–337. https://doi.org/10.1016/j.tim.2016.01.008

Wozniak, D. J., Wyckoff, T. J. O., Starkey, M., Keyser, R., Azadi, P., O'Toole, G. A., & Parsek, M. R. (2003). Alginate is not a significant component of the extracellular polysaccharide matrix of PA14 and PAO1 Pseudomonas aeruginosa biofilms. *Proceedings of the National Academy of Sciences of the United States of America*, *100*(13), 7907–7912. https://doi.org/10.1073/pnas.1231792100

Zheng, H., Korendovych, I. V., & Luk, Y. Y. (2016). Quantification of alginate by aggregation induced by calcium ions and fluorescent polycations. *Analytical Biochemistry*, *492*, 76–81. https://doi.org/10.1016/j.ab.2015.09.016

Zhu, B., Liu, C., Liu, S., Cong, H., Chen, Y., Gu, L., & Ma, L. Z. (2016). Membrane association of SadC enhances its diguanylate cyclase activity to control exopolysaccharides synthesis and biofilm formation in Pseudomonas aeruginosa. *Environmental Microbiology*, *18*(10), 3440–3452. https://doi.org/10.1111/1462-2920.13263

8 Appendix

8.1 R-Code

The R-Code of the statistical analyses of the crystal violet staining (see 2.8.3) is depicted under the following paragraphs.

8.1.1 Preliminary analysis and plotting the data

```
# Reading the data and re-formatting the tables
# ============================================
input_file_path <- "...\\00_Daten\\"
output_file_path <- "...\\20_Bilder\\"
workbook_name <- "Standardkurven_Statistik Sandra.xlsx"
Verd_01 <-
read_excel(paste(input_file_path, workbook_name, sep = ""),
sheet = 1, range = "A1:D12", col_names = T)
Verd_02 <-
read_excel(paste(input_file_path, workbook_name, sep = ""),
sheet = 2, range = "A1:D12", col_names = T)
MessPunkte <- cbind(Verd_01, Verd_02[,2:4])
new_col_names <-
sapply(colnames(MessPunkte)[-1], FUN = function(x){substr(x,15,19)})
tmp <- cbind(c(rep(c("A","B"), each = 3)), new_col_names)
new_col_names <-
apply(tmp,FUN = function(x){paste(x[1], x[2], sep = "_")}, MAR =1)
new_col_names <- c("Konz", new_col_names)
colnames(MessPunkte) <- new_col_names
# Data Table (table_01)
# =====================
xtable(MessPunkte, digits = 3)
# Plotting the data (pic_02)
# ==========================
plot(MessPunkte$Konz, MessPunkte[,2], ylim = c(0,35),
pch = 16, col = rgb(0,0,0,1), xaxt="n",
xlab = "concentration of standard", ylab = "measured value")
xtick <- seq(0, 2, by=0.2)
```

```
axis(side=1, at=xtick, labels = FALSE)
text(x=xtick, y = -1.6,
labels = xtick, pos = 1, xpd = TRUE)
points(MessPunkte$Konz, MessPunkte[,3], pch = 16, col = rgb(1,0,0,1))
points(MessPunkte$Konz, MessPunkte[,4], pch = 16, col = rgb(0,1,0,1))
points(MessPunkte$Konz, MessPunkte[,5], pch = 15, col = rgb(0,0,0,0.3))
points(MessPunkte$Konz, MessPunkte[,6], pch = 15, col = rgb(1,0,0,0.3))
points(MessPunkte$Konz, MessPunkte[,7], pch = 15, col = rgb(0,1,0,0.3))
legend("topleft",
legend =
c("A 18.02.2020","A 19.02.2020","A 10.03.2020",
"B 18.02.2020","B 19.02.2020","B 10.03.2020"),
pch = c(16,16,16,15,15,15),
col =
c(rgb(0,0,0,1),rgb(1,0,0,1),rgb(0,1,0,1),
rgb(0,0,0,0.3),rgb(1,0,0,0.3),rgb(0,1,0,0.3)))
```

8.1.2 Fitting of a polynomial of 2nd degree

```
# Ref-formatting the data
# ======================
data_long <- gather(MessPunkte, "Reihe", "Wert", -Konz)
data_long$VR <- sapply(data_long$Reihe, FUN = function(x){substr(x,1,1)})
data_long$DT <- sapply(data_long$Reihe, FUN = function(x){substr(x,3,7)})
# Regression using a polynomial of degree 3
# ========================================
lm_3 <- lm(Wert ~ Konz + I(Konzˆ2) + I(Konzˆ3) , data = data_long)
b_3 <- lm_3$coef
# table_02:
summary(lm_3)
# table_03:
anova(lm_3)
# Plotting the data (pic_03)
# ==========================
plot(MessPunkte$Konz, MessPunkte[,2], ylim = c(0,35),
pch = 16, col = rgb(0,0,0,1), xaxt="n",
```

```
xlab = "concentration of standard", ylab = "measured value")
xtick <- seq(0, 2, by=0.2)
axis(side=1, at=xtick, labels = FALSE)
text(x=xtick, y = -1.6,
labels = xtick, pos = 1, xpd = TRUE)
points(MessPunkte$Konz, MessPunkte[,3], pch = 16, col = rgb(1,0,0,1))
points(MessPunkte$Konz, MessPunkte[,4], pch = 16, col = rgb(0,1,0,1))
points(MessPunkte$Konz, MessPunkte[,5], pch = 15, col = rgb(0,0,0,0.3))
points(MessPunkte$Konz, MessPunkte[,6], pch = 15, col = rgb(1,0,0,0.3))
points(MessPunkte$Konz, MessPunkte[,7], pch = 15, col = rgb(0,1,0,0.3))
plot_lm_3 <- function(x){b_3[1] + b_3[2] * x + b_3[3] * x^2 + b_3[4] * x^3}
curve(plot_lm_3, 0,2, add = T, col = "red")
legend("topleft",
legend = c("A 18.02.2020","A 19.02.2020","A 10.03.2020",
"B 18.02.2020","B 19.02.2020","B 10.03.2020"),
pch = c(16,16,16,15,15,15),
col = c(rgb(0,0,0,1),rgb(1,0,0,1),rgb(0,1,0,1),
rgb(0,0,0,0.3),rgb(1,0,0,0.3),rgb(0,1,0,0.3)))
# Plotting the polynomial on a larger range (pic_04)
# ================================================
curve(plot_lm_3, 0,6, col = "red",
xlab = "concentration of standard", ylab = "measured value")
# Regression using a polynomial of degree 2
# ========================================
lm_2 <- lm(Wert ~ Konz + I(Konz^2), data = data_long)
b_2 <- lm_2$coef
summary(lm_2)
# Plotting the data (pic_05)
# ==========================
plot(MessPunkte$Konz, MessPunkte[,2], ylim = c(0,35), xlim = c(0,2),
pch = 16, col = rgb(0,0,0,1), xaxt="n",
xlab = "concentration of standard", ylab = "measured value")
xtick <- seq(0, 2, by=0.2)
axis(side=1, at=xtick, labels = FALSE)
```

```
text(x=xtick, y = -1.6,
labels = xtick, pos = 1, xpd = TRUE)
points(MessPunkte$Konz, MessPunkte[,3], pch = 16, col = rgb(1,0,0,1))
points(MessPunkte$Konz, MessPunkte[,4], pch = 16, col = rgb(0,1,0,1))
points(MessPunkte$Konz, MessPunkte[,5], pch = 15, col = rgb(0,0,0,0.3))
points(MessPunkte$Konz, MessPunkte[,6], pch = 15, col = rgb(1,0,0,0.3))
points(MessPunkte$Konz, MessPunkte[,7], pch = 15, col = rgb(0,1,0,0.3))
plot_lm_3 <- function(x){b_3[1] + b_3[2] * x + b_3[3] * x^2 + b_3[4] * x^3}
plot_lm_2 <- function(x){b_2[1] + b_2[2] * x + b_2[3] * x^2}
curve(plot_lm_3, 0,4, add = T, col = rgb(1,0,0,1))
curve(plot_lm_2, 0,4, add = T, col = rgb(0,0,1,1))
# Regression using a polynomial of degree 2
# ========================================
lm_10 <- lm(Wert ~ Konz + I(Konz^2) + I(Konz^3) + I(Konz^4) + I(Konz^5) +
I(Konz^6) + I(Konz^7) + I(Konz^8) + I(Konz^9) + I(Konz^10), data = data_long)
b_10 <- lm_10$coef
summary(lm_10)
# Plotting the data (pic_06)
# ==========================
plot(MessPunkte$Konz, MessPunkte[,2], ylim = c(-10,100),
pch = 16, col = rgb(0,0,0,1), xaxt="n",
xlab = "concentration of standard", ylab = "measured value")
xtick <- seq(0, 2, by=0.2)
axis(side=1, at=xtick, labels = FALSE)
text(x=xtick, y = -15,
labels = xtick, pos = 1, xpd = TRUE)
points(MessPunkte$Konz, MessPunkte[,3], pch = 16, col = rgb(1,0,0,1))
points(MessPunkte$Konz, MessPunkte[,4], pch = 16, col = rgb(0,1,0,1))
points(MessPunkte$Konz, MessPunkte[,5], pch = 15, col = rgb(0,0,0,0.3))
points(MessPunkte$Konz, MessPunkte[,6], pch = 15, col = rgb(1,0,0,0.3))
points(MessPunkte$Konz, MessPunkte[,7], pch = 15, col = rgb(0,1,0,0.3))
plot_lm_10 <- function(x){b_10[1] +
b_10[2] * x +
b_10[3] * x^2 +
```

```
b_10[4] * xˆ3 +
b_10[5] * xˆ4 +
b_10[6] * xˆ5 +
b_10[7] * xˆ6 +
b_10[8] * xˆ7 +
b_10[9] * xˆ8 +
b_10[10] * xˆ9 +
b_10[11] * xˆ10 }
curve(plot_lm_10, 0,2, add = T, col = "red")
```

8.1.3: Confidence and prediction bands

```
# Confidence Bands
# ================
plot(MessPunkte$Konz, MessPunkte[,2], ylim = c(0,35), xlim = c(0,2),
pch = 16, col = rgb(0,0,0,1), xaxt="n",
xlab = "concentration of standard", ylab = "measured value")
xtick <- seq(0, 2, by=0.2)
axis(side=1, at=xtick, labels = FALSE)
text(x=xtick, y = -1.6,
labels = xtick, pos = 1, xpd = TRUE)
points(MessPunkte$Konz, MessPunkte[,3], pch = 16, col = rgb(1,0,0,1))
points(MessPunkte$Konz, MessPunkte[,4], pch = 16, col = rgb(0,1,0,1))
points(MessPunkte$Konz, MessPunkte[,5], pch = 15, col = rgb(0,0,0,0.3))
points(MessPunkte$Konz, MessPunkte[,6], pch = 15, col = rgb(1,0,0,0.3))
points(MessPunkte$Konz, MessPunkte[,7], pch = 15, col = rgb(0,1,0,0.3))
plot_lm_2 <- function(x){b_2[1] + b_2[2] * x + b_2[3] * xˆ2}
curve(plot_lm_2, 0,2, add = T, col = rgb(0,0,1,1))
predicted.intervals <-
predict(lm_2,data.frame(Konz=seq(0,2,0.1)),interval='confidence', level=0.95)
lines(seq(0,2,0.1),predicted.intervals[,2],col='red',lwd=2)
lines(seq(0,2,0.1),predicted.intervals[,3],col='red',lwd=2)
# Prediction band
# ===============
plot(MessPunkte$Konz, MessPunkte[,2], ylim = c(0,35), xlim = c(0,2),
pch = 16, col = rgb(0,0,0,1), xaxt="n",
```

```
xlab = "concentration of standard", ylab = "measured value")
xtick <- seq(0, 2, by=0.2)
axis(side=1, at=xtick, labels = FALSE)
text(x=xtick, y = -1.6,
labels = xtick, pos = 1, xpd = TRUE)
points(MessPunkte$Konz, MessPunkte[,3], pch = 16, col = rgb(1,0,0,1))
points(MessPunkte$Konz, MessPunkte[,4], pch = 16, col = rgb(0,1,0,1))
points(MessPunkte$Konz, MessPunkte[,5], pch = 15, col = rgb(0,0,0,0.3))
points(MessPunkte$Konz, MessPunkte[,6], pch = 15, col = rgb(1,0,0,0.3))
points(MessPunkte$Konz, MessPunkte[,7], pch = 15, col = rgb(0,1,0,0.3))
plot_lm_2 <- function(x){b_2[1] + b_2[2] * x + b_2[3] * x^2}
curve(plot_lm_2, 0,2, add = T, col = rgb(0,0,1,1))
predicted.intervals <-
predict(lm_2,data.frame(Konz=seq(0,2,0.1)),interval='prediction', level=0.95)
lines(seq(0,2,0.1),predicted.intervals[,2],col='red',lwd=2)
lines(seq(0,2,0.1),predicted.intervals[,3],col='red',lwd=2)
```

8.1.4 Linear regression

```
# Calibration curve
# =================
# interlude_ linear regression
# with dummy variable (picture 10)
tmp <- which(data_long$Konz <= 0.8)
p <- ggplot(data = data_long[tmp,], aes(x= Konz, y = Wert)) +
geom_point(aes(colour = as.factor(VR)), size = 1) +
geom_smooth(method = "lm", se=FALSE, formula = y ~ x, aes(colour=as.factor(VR))) +
xlab("concentration of standard") +
ylab("measured value") +
labs(color = "experimental setting")
p
# table_07
anova(lm(Wert ~ Konz + VR, data = data_long[tmp,]))
# without dummy variable
lm_1 <- lm(Wert ~ Konz, data = data_long[tmp,])
# table_08
```

```
summary(lm_1)
df_lm <- data.frame(Konz = seq(0, 0.8, 0.025))
df_lm$Wert <- predict(lm_1, newdata = df_lm)
df_lm$p_low <- predict(lm_1, newdata = df_lm, interval='prediction', level=0.95)[,2]
df_lm$p_up <- predict(lm_1, newdata = df_lm, interval='prediction', level=0.95)[,3]
df_lm$c_low <- predict(lm_1, newdata = df_lm, interval='confidence', level=0.95)[,2]
df_lm$c_up <- predict(lm_1, newdata = df_lm, interval='confidence', level=0.95)[,3]
# picture 11
ggplot(data_long[tmp,], aes(x = Konz, y = Wert)) +
geom_point() +
xlab("concentration of standard") +
ylab("measured value") +
geom_line(data = df_lm , aes(x = Konz, y = Wert), colour = "black") +
geom_line(data = df_lm , aes(x = Konz, y = p_low), colour = "blue") +
geom_line(data = df_lm , aes(x = Konz, y = p_up), colour = "blue") +
geom_line(data = df_lm , aes(x = Konz, y = c_low), colour = "red") +
geom_line(data = df_lm , aes(x = Konz, y = c_up), colour = "red")
# calibration interval
# picture_12
library(investr)
lm_1 <- lm(Wert ~ Konz, data = data_long[tmp,])
res_est <- sapply(seq(0,10,0.25),
FUN = function(y0){calibrate(lm_1, y0,
interval = "inversion", level = 0.95)$estimate})
res_lwr <- sapply(seq(0,10,0.25),
FUN = function(y0){calibrate(lm_1, y0,
interval = "inversion", level = 0.95)$lower})
res_upr <- sapply(seq(0,10,0.25),
FUN = function(y0){calibrate(lm_1, y0,
interval = "inversion", level = 0.95)$upper})
data_table <- data.frame("Messwerte" = seq(0,10,0.25),
"Konzentration" = round(res_est,2),
"untere 95%-Grenze" = round(res_lwr,2),
"obere 95%-Grenze" = round(res_upr,2))
```

```
plot(seq(0,10,0.25), res_est, type = "l",
xlab = "measured value", ylab = "concentration", ylim = c(0,0.6))
points(seq(0,10,0.25), res_lwr, type = "l", col = "blue")
points(seq(0,10,0.25), res_upr, type = "l", col = "blue")
```

8.2 Results of the statistical tests

Table 7: Coefficients of a polynomial of 2nd degree fitted to the data by regression analysis

	Estimate	Standard Error	t value	$P_r(>\|t\|)$
a_0	0,5669	1,5293	0,371	0,712098
a_1	26,3228	3,5576	7,399	4,02e-10
a_2	-6,6634	1,7133	-3,889	0,000245

In Table 7, the coefficients of a polynomial of 2nd degree that was fitted to the data of the crystal violet staining experiments depicted at 3.2.1 are displayed. The t-values and p-values of a t-test are depicted as well. A_0, a_1 and a_2 refer to coefficients of the polynomial of 2nd degree that was fitted to the data. The t value refers to a t-test that was performed, and the $P_r(>|t|)$ refers to its p-value.

Table 8: Coefficients of the linear regression (polynomial of 1st degree)

	Estimate	Standard Error	t value	$P_r(>\|t\|)$
a_0	1,2185	0,6627	1,839	0,0766
a_1	20,4119	1,3527	15,090	5,62e-10

In Table 8, the coefficients of a linear regression that was fitted to the data of the crystal violet staining experiments depicted at 3.2.1 are displayed. The t-values and p-values of a t-test are depicted as well. A_1, and a_2 refer to coefficients of the linear regression that was fitted to the data. The t value refers to a t-test that was performed, and the $P_r(>|t|)$ refers to its p-value.

9 Erklärung zum Eigenanteil

Die Arbeit wurde am Interfakultären Institut für Mikrobiologie und Infektionsmedizin (Tübingen) unter Betreuung von PD Dr. Erwin Bohn durchgeführt.

Die Konzeption des Projekts erfolgte durch Dr. Sandra Schwarz.

Sämtliche Versuche wurden nach Einarbeitung durch Labormitglieder Dr. Sandra Schwarz, Przemek Olejnik und Dr. Jan Lennings von mir durchgeführt. Ein Durchlauf der Alcianblau-Färbung wurde von Dr. Sandra Schwarz durchgeführt, dieser ist unter Figure 17 abgebildet.

Die statistische Auswertung erfolgte durch Dr. Ulrich Schoppmeier, von dem auch die Figures 8, 9 und 10 erstellt wurden. Der R-Code ist im Appendix zu finden.

Ich versichere, das Manuskript selbständig verfasst zu haben und keine weiteren als die von mir angegebenen Quellen verwendet zu haben.

Tübingen, den

[Unterschrift]

10 Danksagung

An dieser Stelle möchte ich mich ganz herzlich bei allen bedanken, die mich bei meiner Promotion unterstützt haben. Vor allem möchte ich mich bei Dr. Sandra Schwarz bedanken, dass sie mir das Projekt ermöglicht und mich immer bei der Durchführung und beim Schreiben unterstützt hat. Bei PD Dr. Erwin Bohn möchte ich mich herzlich für die Übernahme der Betreuung bedanken. Des Weiteren möchte ich mich bei Przemek Olejnik bedanken, der mich in den ersten Wochen eingearbeitet hat und auch danach für Ratschläge und Unterstützung zur Verfügung stand.

Ganz besonders möchte ich mich auch bei Dr. Ulrich Schoppmeier für die ausführliche statistische Analyse, kompetente Beratung und Beantwortung meiner Fragen bedanken.

Zudem möchte ich mich natürlich auch bei Jan Lennings, Isa Samp, Noreen Buhlinger und allen anderen bedanken, die während meiner Zeit im Labor Teil der AG Schwarz waren. Auf eure Unterstützung und euer Fachwissen konnte ich immer zählen und ich habe mich durch das angenehme Arbeitsklima in der Arbeitsgruppe sehr wohl gefühlt.

Als letztes gilt ein besonderer Dank noch meiner Familie und meinen Freund:innen für Ihre Unterstützung.